



STANFORD RESEARCH INSTITUTE  
Menlo Park, California 94025 · U.S.A.

*Final Report*

*April 16, 1976*

## THE RESPONSE OF SMOKE DETECTORS TO PYROLYSIS AND COMBUSTION PRODUCTS FROM AIRCRAFT INTERIOR MATERIALS

*By:* ROBERT G. McKEE  
NORMAN J. ALVARES

*Prepared for:*

NATIONAL AERONAUTICS AND SPACE ADMINISTRATION  
AMES RESEARCH CENTER  
MOFFETT FIELD, CALIFORNIA 94035

CONTRACT NAS2-8583

SRI Project PYU-3830

*Approved by:*

RUSSELL C. PHILLIPS, *Director*  
*Chemical Engineering Laboratory*

PAUL J. JORGENSEN, *Executive Director*  
*Physical Sciences Division*

## CONTENTS

LIST OF ILLUSTRATIONS . . . . .	iii
LIST OF TABLES . . . . .	iv
I INTRODUCTION . . . . .	1
II DETECTOR SELECTION AND DESIGN . . . . .	4
Detector Selection Criteria . . . . .	4
Apparatus Design . . . . .	6
Instrumentation . . . . .	6
III TESTING . . . . .	16
Test Procedure . . . . .	17
Results and Discussion . . . . .	18
Radiant Heat Exposure of Group I Materials . . . . .	23
Flame Exposure of Group I Materials . . . . .	29
Heated Coil Exposure of Group II Materials . . . . .	35
Radiant Heat Exposure of Group III Materials . . . . .	36
Air Velocity, Humidity, and Ambient Pressure Effects on Detector Performance . . . . .	39
Conclusions . . . . .	42
APPENDICES	
A SUGGESTED OVERALL PROGRAM FOR THE DEVELOPMENT OF FIRE DETECTORS FOR COMMERCIAL AIRCRAFT . . . . .	46
B SURVEY OF ACTUAL FIRE DETECTION IN AIRCRAFT FUSELAGE AREAS . . . . .	49
REFERENCES . . . . .	50

## ILLUSTRATIONS

1	Schematic Flow Chart of Test Circuitry . . . . .	7
2	Detector Layout . . . . .	8
3	Photographs of Test Chamber and Recording Station . . . . .	9
4	Exterior and Interior Views of Pyrolizing Furnace . . . . .	11
5	Exterior and Interior Views of Pyrolizing Furnace. . . . .	12
6	Schematic Drawing of Radiant Heat Source Showing Lamp Mounting Details . . . . .	13
7	Irradiance Versus Distance from the Front Bank of Lamps of the Radiant Source . . . . .	14
8	Test 57: Reproduction of Oscillograph Record . . . . .	17
9	Test 57: Polyester Glass Laminate . . . . .	18
10	Test 106: Polyester Glass Laminate . . . . .	19
11	Test 195: Epoxy Glass Faces, Nomex Core . . . . .	20
12	Composite Averaged Optical Transmission for Various Group I Materials Tested . . . . .	28
13	Plot of $O_u^*$ Versus $\bar{v}$ for Pyrotector SK 700 LED Smoke Detector . . . . .	40
14	Plot of $O_u^*$ Versus $\bar{v}$ for PYR-A-Larm D1-2S Ionization Detector . . . . .	41
15	Pressure and Humidity Chamber . . . . .	43

TABLES

1	Materials Grouped by Exposure Source . . . . .	3
2	Detectors Selected for Evaluation . . . . .	5
3	Detector Actuation Summary . . . . .	22
4	Group I Radiant Heat Exposure: Detector Response Data . . . . .	24
5	Group I Radiant Heat Exposure: Order of Detector Actuation . . . . .	26
6	Group I Radiant Heat Exposure: Optical Density at Detector Actuation . . . . .	30
7	Group I Materials: Preliminary Flame Tests . . . . .	32
8	Group I Flame Exposure and Group II Heated Coil Exposure: Order of Detector Actuation . . . . .	33
9	Group I Flame Exposure and Group II Heated Coil Exposure: Optical Density at Detector Actuation . . . . .	34
10	Group III Radiant Heat Exposure: Order of Detector Actuation . . . . .	36
11	Group III Radiant Heat Exposure: Optical Density at Detector Actuation . . . . .	37
12	Selected Detectors at Elevated Humidity and Reduced Pressure . . . . .	44

## I INTRODUCTION

Under contract to NASA, Ames Research Laboratories, Stanford Research Institute (SRI) conducted the passenger compartment detector phase of a program which is developing and testing economically feasible fire-resistant materials for interior furnishings and finishes of aircraft and also developing active on-board fire protection measures including early detection of incipient fires in passenger and cargo compartments. The tasks of our phase of the program were to:

- (1) Determine the sensitivity of contemporary gas and smoke detectors to pyrolysis and combustion products from materials commonly used in aircraft interiors and from materials that may be used in the future. NASA selected the materials to be tested.
- (2) Assess environmental limitations to detector sensitivity and reliability.
- (3) Evaluate the compatibility of the tested detectors with the passenger cabins of commercial aircraft.
- (4) Select and install the optimum detectors in full-scale lavatory modules during burnout tests at the University of California Fire Testing Facility at Richmond, California.

In mutual agreement with NASA, Task 3 was excluded from the scope of this part of the investigation. It may be the subject of a proposal for continued work in the future.

After evaluation of the test conditions during the lavatory module burn-out tests at the University of California Fire Testing Facility, NASA representatives, SRI staff, and U.C. personnel concluded that the data received from participation in these tests, as described in Task 4, would be of questionable value. Consequently, Task 4 was not conducted.

Task 2 was done simultaneously with the Task 1 testing program. Both tasks have been completed and are discussed in more detail later in the report.

The tests were conducted on three groups of materials by exposure to three sources of ignition. The materials were divided according to those that were easily obtainable and advanced materials not readily available. The three sources of exposure used to test the materials are:

- Radiant and Meeker burner flame
- Heated coil
- Radiant source only.

Table 1 lists the three groups of materials tested by the source of exposure.

The first test series used radiant heat and flame exposures on easily obtained test material. In the second test series, four materials were selected from the first group and exposed to an incandescent coil to provide the conditions for smoldering combustion. Only cellulose-based materials were coil-tested because only they would reproducibly respond in a smoldering mode.

The third test series used only radiant heat exposures on advanced materials that were not readily available. A significant time period was required to collect sufficient quantities for replicate testing. Despite the time expended, some of the materials were so scarce or expensive that only enough were allotted for testing in one exposure.

Table 1

MATERIALS GROUPED FOR DETECTOR TESTING BY EXPOSURE SOURCE

Group I: Radiant Heat Source and Meeker Burner Flame

Polyurethane foam 0.048 g/cm<sup>3</sup>  
Polyurethane foam 0.032 g/cm<sup>3</sup>  
Polyethylene foam 0.032 g/cm<sup>3</sup>  
100% Cotton fabric  
100% Wool fabric  
50% Cotton/50% rayon fabric  
100% Wool carpet with latex backing  
Modacrylic carpet with latex backing  
Acrylonitrile butadiene styrene (molded)  
Lexan (clear)  
Paper towel  
Kleenex  
Polyethylene (film)  
Polyethylene (cast)  
Polyester glass laminate  
Polystyrene (cast)  
Polystyrene cups

Group II: Heated Coil

100% Cotton fabric  
50% Cotton/50% rayon fabric \*  
Paper towel  
Kleenex

Group III: Radiant Heat Source Only

Acrylonitrile butadiene styrene (ABS)  
Chlorinated polyvinyl chloride (PVC)  
Polycarbonate  
Polybenzimidazol fabric (FBI)  
Kynol cloth  
Polyether sulfone  
New L.S. polycarbonate F-6000  
Modified polyphenylene oxide (Noryl)  
Metcon  
Modified Polysulfone  
Polyphenylene sulfide  
Nomex fabric (RT40-90)  
Silicone elastomer  
Epoxy glass faces, Nomex core  
Tedlar-coated phenolic glass faces, Nomex core  
Tedlar-coated phenolic glass laminate  
Tedlar, PVC film  
Fire-retardant polyurethane foam  
Neoprene with cord filler

\* Material subjected to elevated humidity and reduced pressure environments.

## II DETECTOR SELECTION AND DESIGN

### Detector Selection Criteria

Because of the critical need to detect the incipient fire as soon as possible after initiation, only detectors that sense combustion gases or aerosols were selected for comparative evaluation. Our initial approach was to identify smoke detectors that major airlines currently use for cargo hold and galley fire protection. This effort was not fruitful because of a lack of information (see Appendix B). Therefore, detectors were chosen from the generic classes of ionization, photo-electric, and gas-sensing instruments currently available as off-the-shelf units. Detector selection procedures required that the unit be marketed by the manufacturer or have an established record of reliability and sensitivity. Before an instrument was purchased or borrowed from a manufacturer, its characteristics and capabilities were discussed with national experts on fire detectors.

We are aware that this selection procedure appears to be somewhat arbitrary. To complete the goals of the program within the cost constraints of the contract, however, this part of the effort had to be completed as expeditiously as possible. We believe that the results obtained with the selected detectors can be translated to the response of similar, first quality detectors, not included in these tests, but of the same generic class. That is, all ionization detectors should be reliable in detecting fire gases sensed by the selected ionization detectors used in these tests.

The detectors selected for the survey and the numbers used to identify them during testing are listed on Table 2. Before the third series of

Table 2

## DETECTORS SELECTED FOR EVALUATION

Assigned Number	Name	Manufacturer	Type
D1	Save-A-Life (No. 525)	KF Industries	Gas sensor
D2	Guardion (FRU-1)	Pyrotronics	Ionization
D3	Smoke and Heat Detector (30-290-9)	Pyrotronics	Photoelectric
D4	724-L Detector	Electro-Signal Laboratory	Photoelectric
D5	824-L Detector	Electro-Signal Laboratory	Photoelectric
D6	EM-6 Detector	Cerberus	Ionization
D7	RM-6 Detector	Cerberus	Photoelectric
D8 <sup>*</sup>	Smoke and Heat Detector (30-231-30)	Pyrotector	Photoelectric
D9 <sup>†</sup>	Smoke Detector	Celesco/Pyrotronics	Ionization

\* Detector added for Group I flame exposure tests and Group III tests.

† Detector added for Group III tests. Detector has two alarms (rate and level) denoted in tables that follow as D9R (rate) D9L (level).

tests were undertaken, NASA requested that the Celesco detector be added to the set of detectors initially selected.

### Apparatus Design

Recording the response of nine smoke detectors exposed to products from up to forty different materials with sufficient replications of each material exposure to provide statistical significance is formidable. The complexity of the task was increased by the requirement that detector response be appraised for pyrolysis and for both flaming and smoldering ignition modes. Thus, the testing apparatus had to provide uniform and repeatable conditions during exposures and had to be simple enough that the test recycle time would be relatively short.

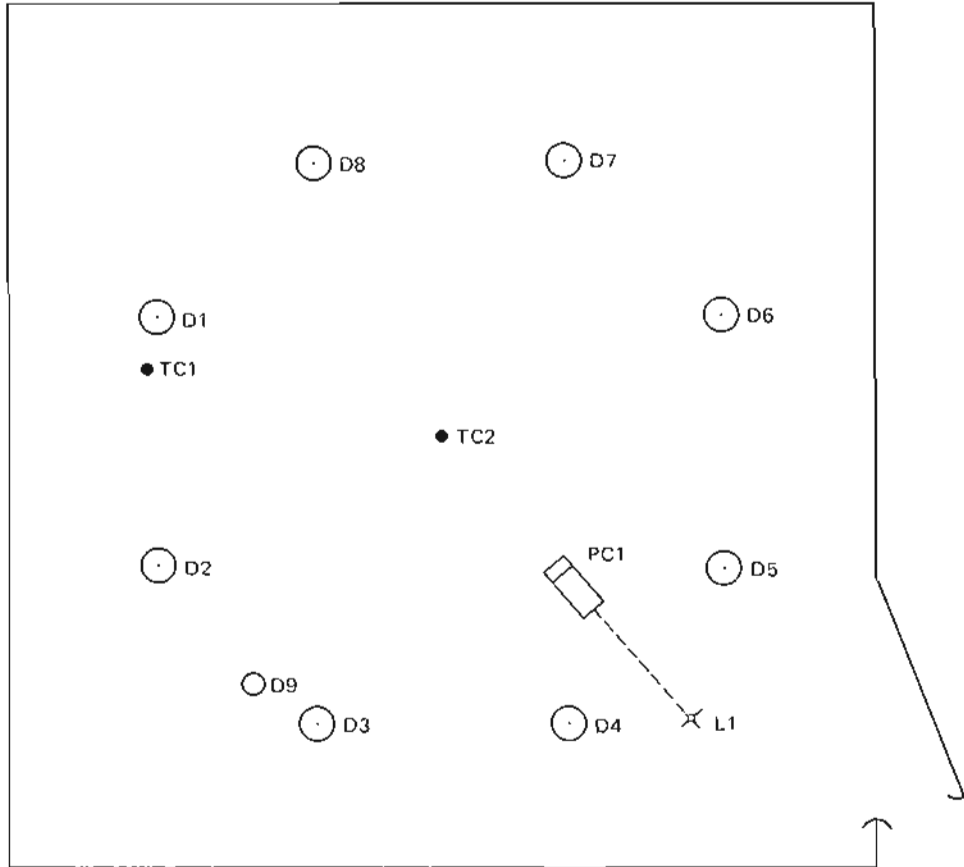
The apparatus shown schematically in Figure 1 was designed and constructed with these constraints in mind. This design is based on one that Factory Mutual used to compare detectors for a HUD project.<sup>1</sup> In these initial tests, smoke from radiantly heated, pyrolyzing material is accelerated through a smoke pipe by an air ejector jet to the center of the ceiling of the test enclosure, where it spreads radially from the pipe. The detectors are located in a circular array equidistant from the center. A meter to measure the light transmission across a 30.5-cm path in line with the smoke flow and several thermocouples complete the sensor array. The schematic identifies the locations of the sensors and their circuit path to the recording instruments and power supplies. Figure 2 details the detector configuration for the tests with the Group III materials. Photographs of the test enclosure and attendant electronics are shown in Figure 3.

### Instrumentation

The measurements for each test were recorded on a 36-channel recorder. Signals were measured from thermocouples, detector alarm event markers, the smoke density meter, and an electronic load cell that measured specimen weight loss during exposure.



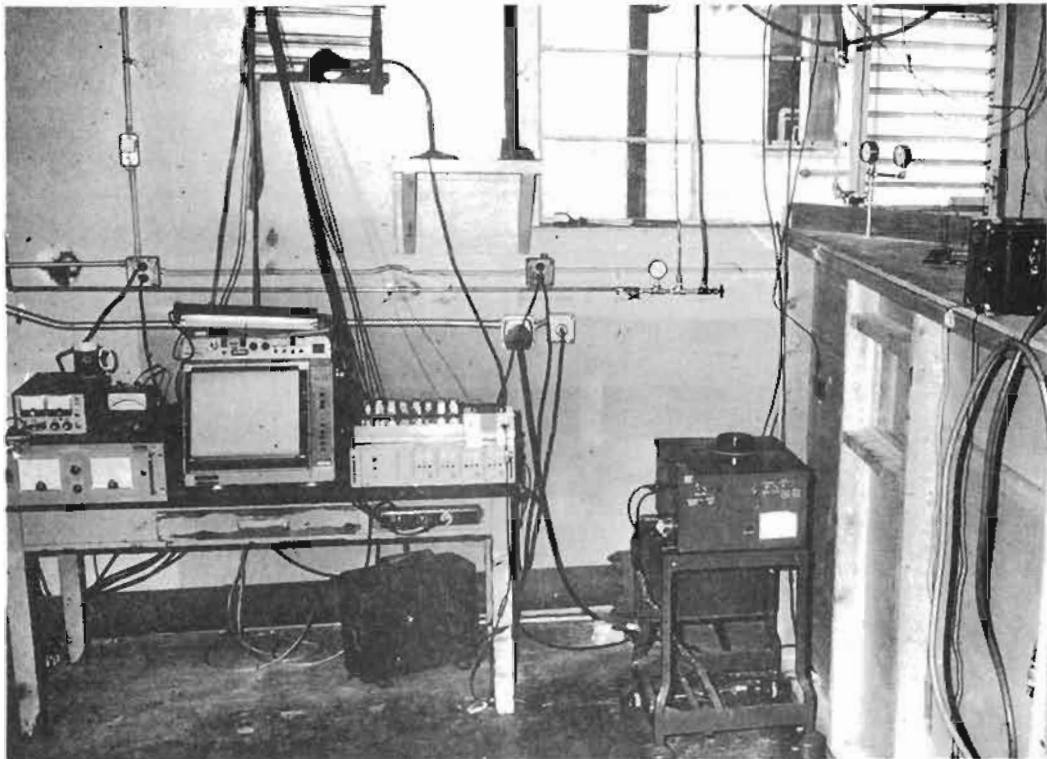
DETECTOR LAYOUT



- TC1 - Detector Ring Thermocouple
- TC2 - Smoke Exhaust Thermocouple
- PC1 and L1 - Transmission Meter
- D1 - KF Gas Cell (Save-a-life No. 525)
- D2 - Pyrotronics Ionization (Guardian FRU-1)
- D3 - Pyrotector (Smoke and Heat Detector 30-290-9)
- D4 - ESL Photoelectric (Commercial No. 724)
- D5 - ESL Photoelectric (Experimental No. 824)
- D6 - Cerberus Ionization (FM-6)
- D7 - Cerberus Photoelectric (RM-6)
- D8 - Pyrotector Type II (30-231-30)
- D9 - Celesco (CII Prototype)

SA-3830-10

FIGURE 2 DETECTOR LAYOUT



SA-3830-8

FIGURE 3 PHOTOGRAPHS OF TEST CHAMBER AND RECORDING STATION

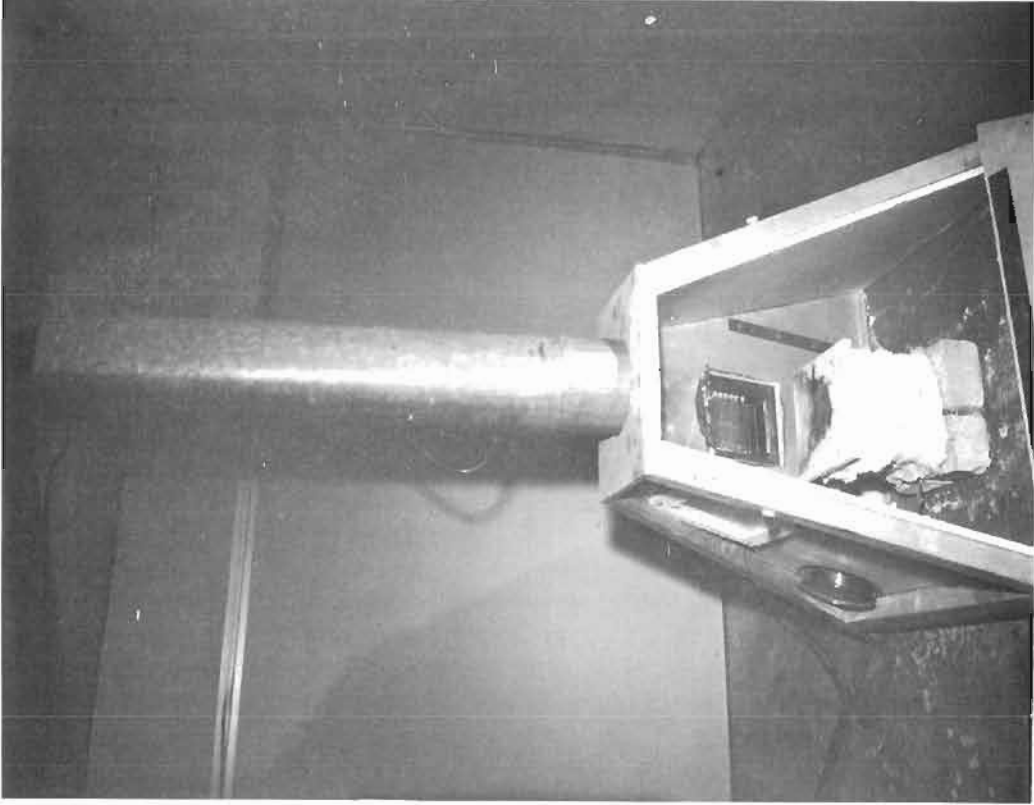
The thermocouples are denoted as TC1, TC2, and TC3. The first two thermocouples measure the temperature at the following locations: TC1 at the detector circle and TC2 at the smoke pipe exhaust. The third thermocouple, TC3, was placed close to the radiant source in the smoke generator to obtain on-off time. Thermocouples TC1 and TC2 were calibrated electrically by applying known mV signals in series with the thermocouple and galvanometric circuit. Thermocouple, TC3 was not calibrated because it was used only as an event marker to establish a zero time reference. Thermocouple reference junctions were all maintained at 0°C.

Smoke density was measured by using a photovoltaic cell in conjunction with a foot-candle meter and light source. The output from the cell was applied to the foot-candle meter and recorded by the oscillograph. The intensity of the light source was adjusted so that 100 foot-candles represented 100% transmission, 50 foot-candles represented 50% transmission, and so on. The response of the photocell is linear.

The weight loss of the tested materials was obtained with an electronic load cell. Potential errors caused by heat absorption from the radiant heat and flame sources were eliminated by mounting the load cell unit in an insulated container as illustrated in the right-hand picture of Figure 4. The output signal of the load cell was applied to a bucking voltage circuit to offset the platform and sample holder weight.

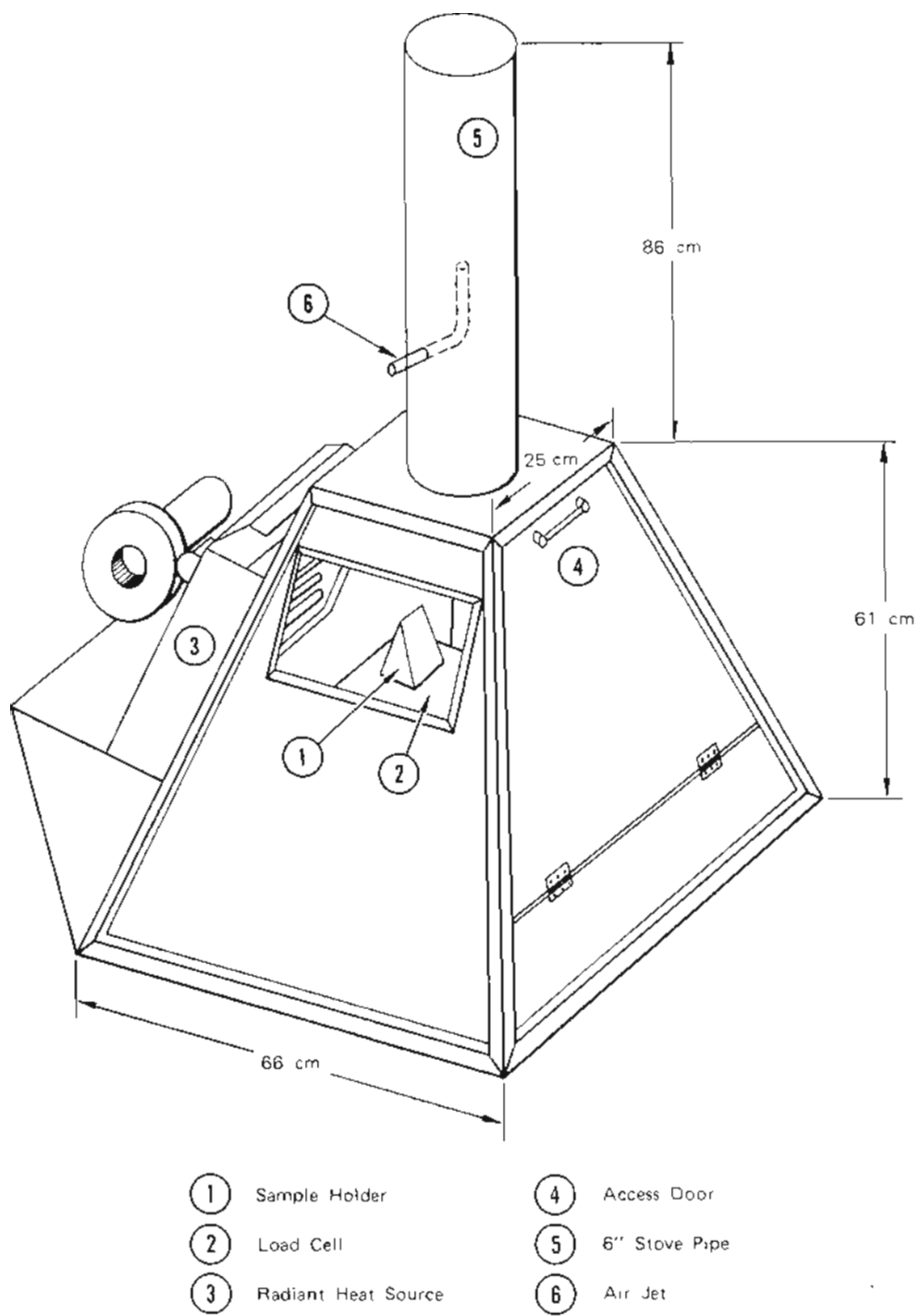
Figure 5 is a schematic of the smoke generator showing the relative positions of the radiant heat source, the specimen exposure plane, the load cell, and the air ejector. Photographs of the generator are shown in Figure 4. Also visible in these pictures are some of the detectors in their normal positions on the detector ring.

Figure 6 is a schematic of the radiant heat source used for the pyrolysis studies. Figure 7 shows the radiant energy variation with distance.



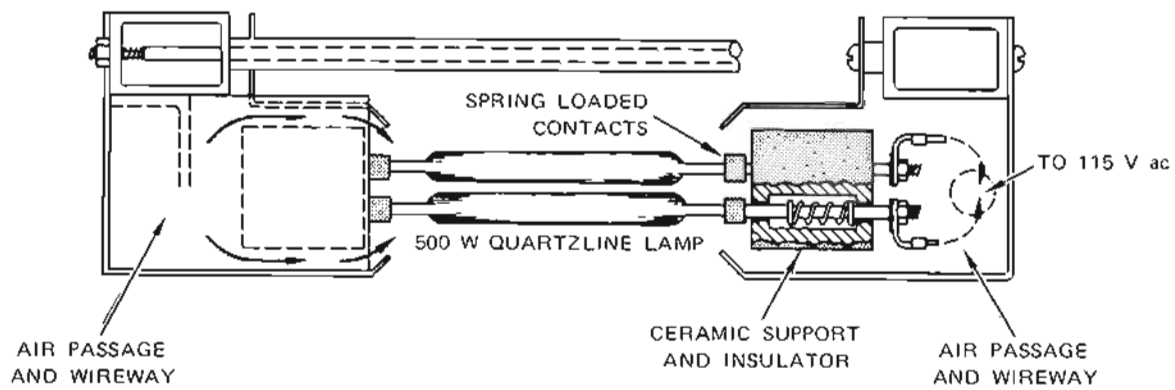
SA-3830-7

FIGURE 4 EXTERIOR AND INTERIOR VIEWS OF PYROLIZING FURNACE

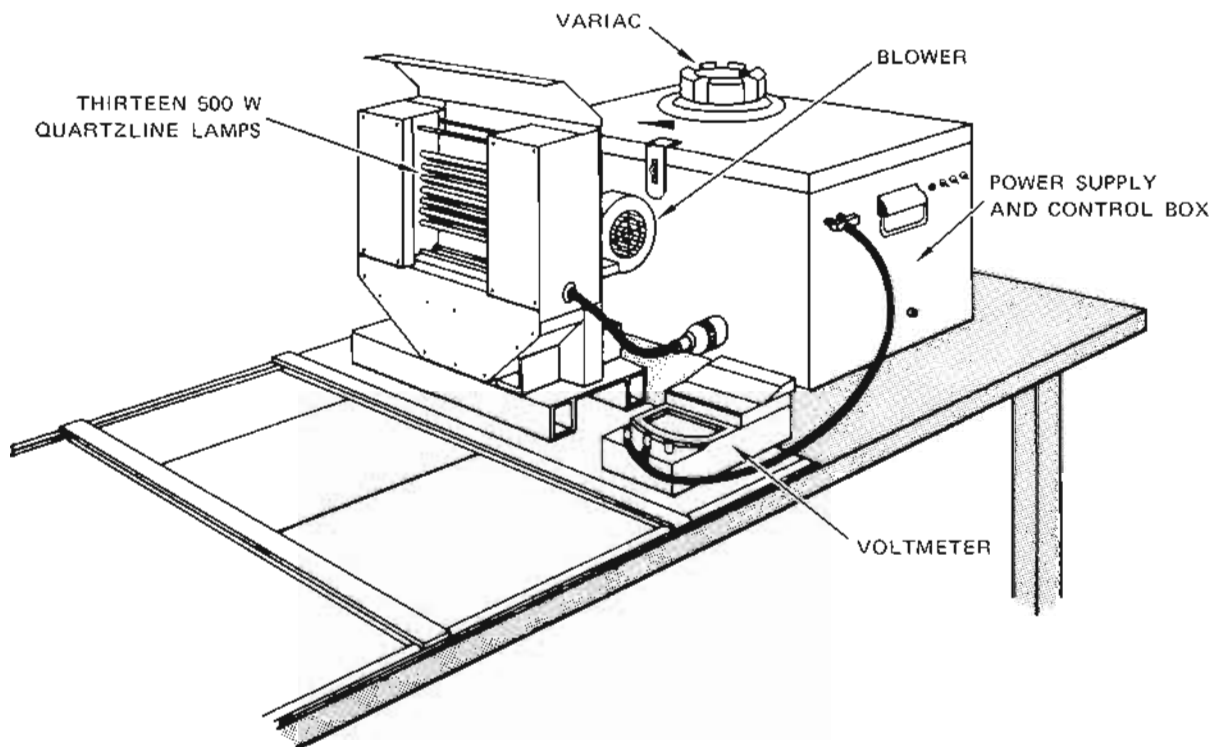


SA-3830-2

FIGURE 5 EXTERIOR AND INTERIOR VIEWS OF PYROLIZING FURNACE

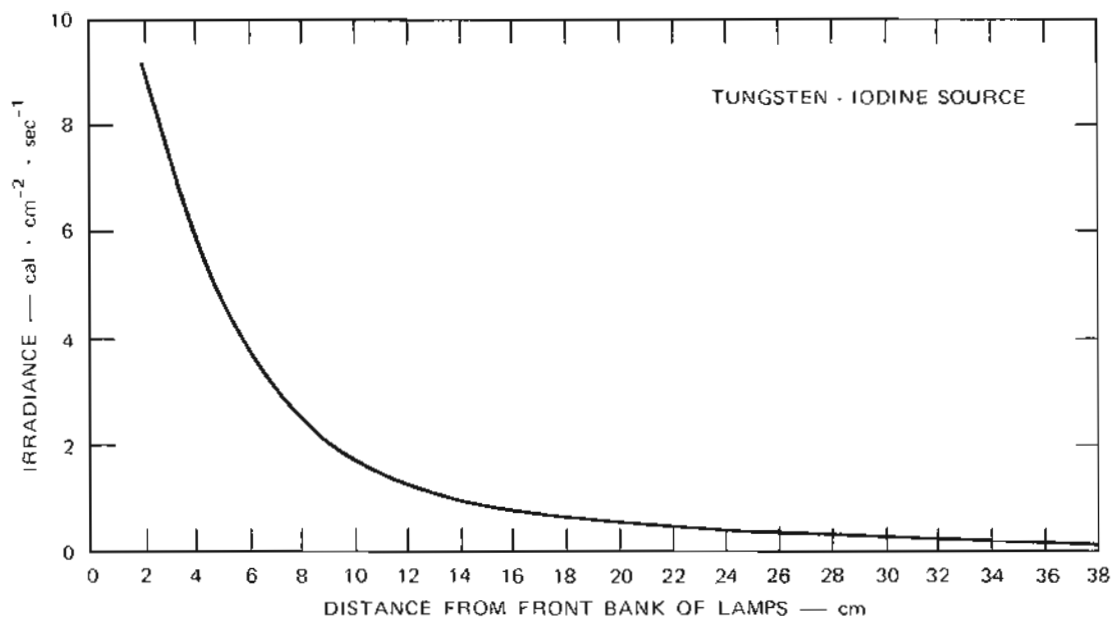


DETAIL OF QUARTZLINE LAMP



SA-3830-3

FIGURE 6 SCHEMATIC DRAWING OF RADIANT HEAT SOURCE SHOWING LAMP MOUNTING DETAILS



SA-3830-4

FIGURE 7 IRRADIANCE VERSUS DISTANCE FROM THE FRONT BANK OF LAMPS OF THE RADIANT SOURCE

Flame exposures were conducted with a Meeker burner located in place of the radiant heat source. The burner flame (premixed natural gas at a flow rate of 1.0 CFM) was directed to contact the test specimen in the same orientation as the radiant heat exposure tests.

To ensure that the combustion products of the burner flame would not alarm the detectors, the burner was positioned approximately 5 to 6 cm directly beneath each detector. None of the detectors indicated an alarm state. It was noted that D1 alarmed on unburned natural gas; however, it was the only detector to exhibit this response.

Smoldering exposures were made by placing selected test specimens (those that would smolder easily) on a glowing heating coil until the specimens started smoldering. No weight loss data were obtained during these tests since the mass of fuel was small relative to the weight of the heating coils, and the entire system was beyond the range of the load cell.

### III TESTING

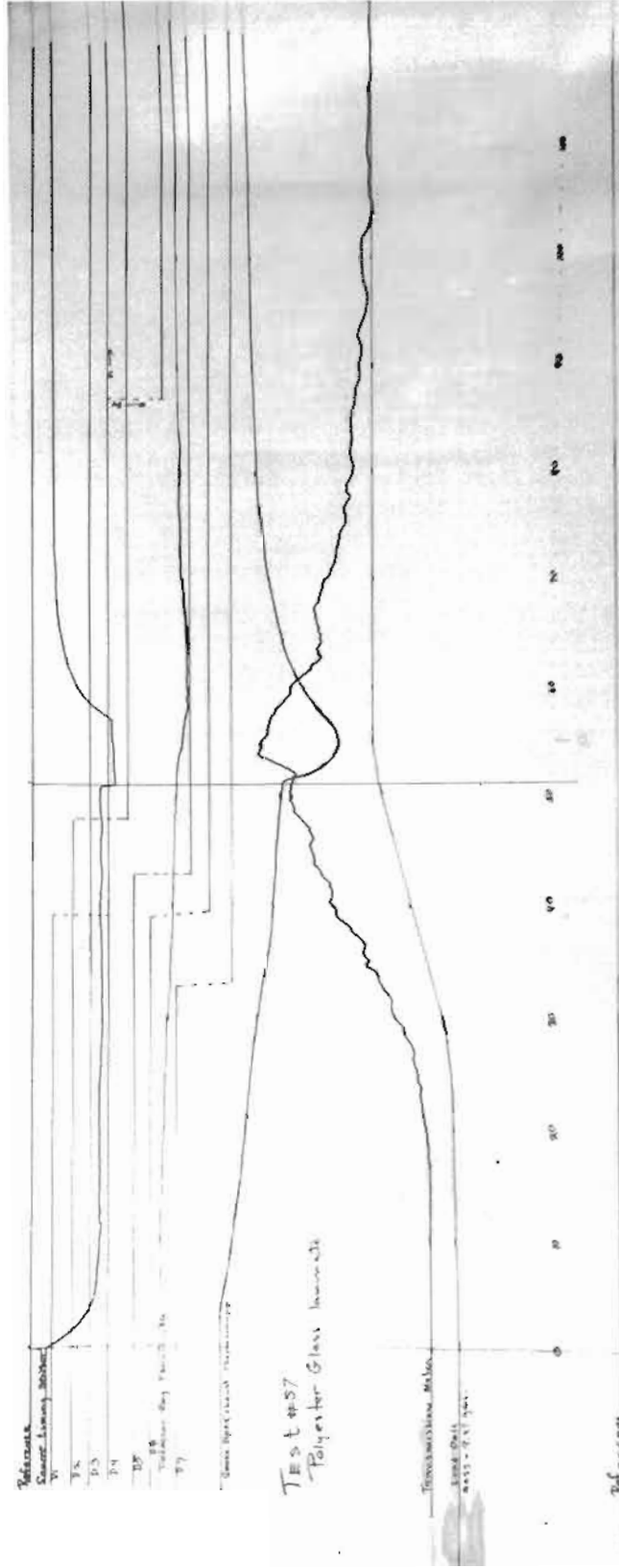
#### Test Procedure

The detectors were exposed to the pyrolysis products from 36 materials, the combustion products from 17 materials, and the smoldering combustion products from 4 materials. To ensure uniformity of test conditions, the testing day began and ended with a calibration test using a standard flexible polyurethane foam (density  $0.048 \text{ g/cm}^3$ ) that would actuate all detectors on pyrolysis. Each material, except those difficult to obtain, was tested three or more times to obtain some statistical relevance in the response data. A pattern for preexposure conditioning and post-exposure cleaning was repeated for each exposure.

#### Results and Discussion

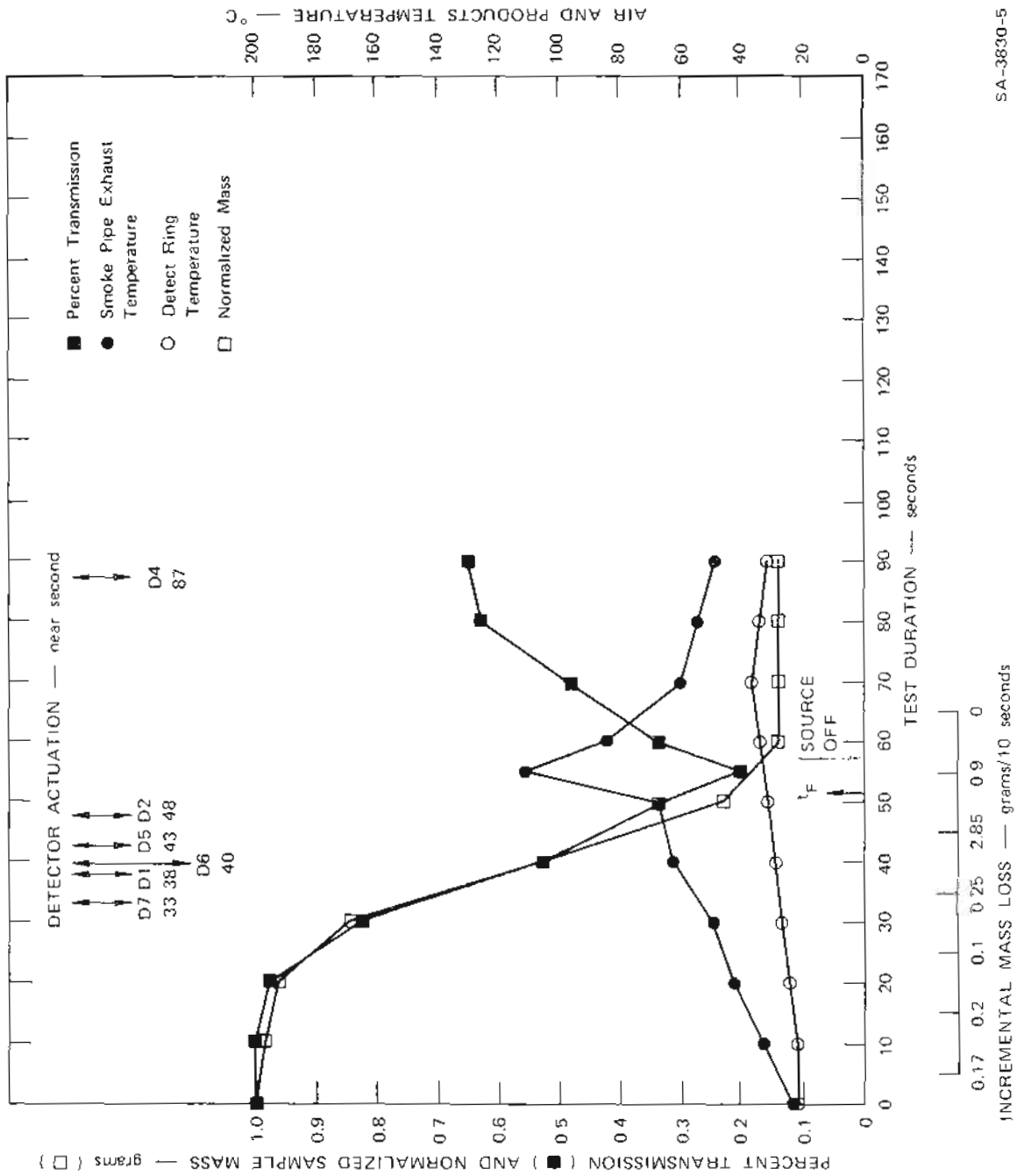
Figure 8 shows an oscillograph record for Test 57 in which polyester glass laminate was exposed to an irradiance of  $2.15 \text{ cal cm}^{-2} \text{ sec}^{-1}$  (approximately 8 W). The individual galvanometer traces are identified, and the time increments for data reduction are included at the bottom of the record. Figure 9 gives the reduced data from the record shown in Figure 8. The data from each test are reduced to this form. These figures contain essentially all the information recorded during the test except the environmental conditions.

The reduced data curves for a flame exposure of polyester glass laminate (Test 106) are shown in Figure 10, and those for a radiant exposure for a composite panel consisting of epoxy glass faces with a Nomex honeycomb core (Test 195) are shown in Figure 11. These data illustrate the response characteristics common to different exposure modes and material design. Essentially, the test durations are shorter for



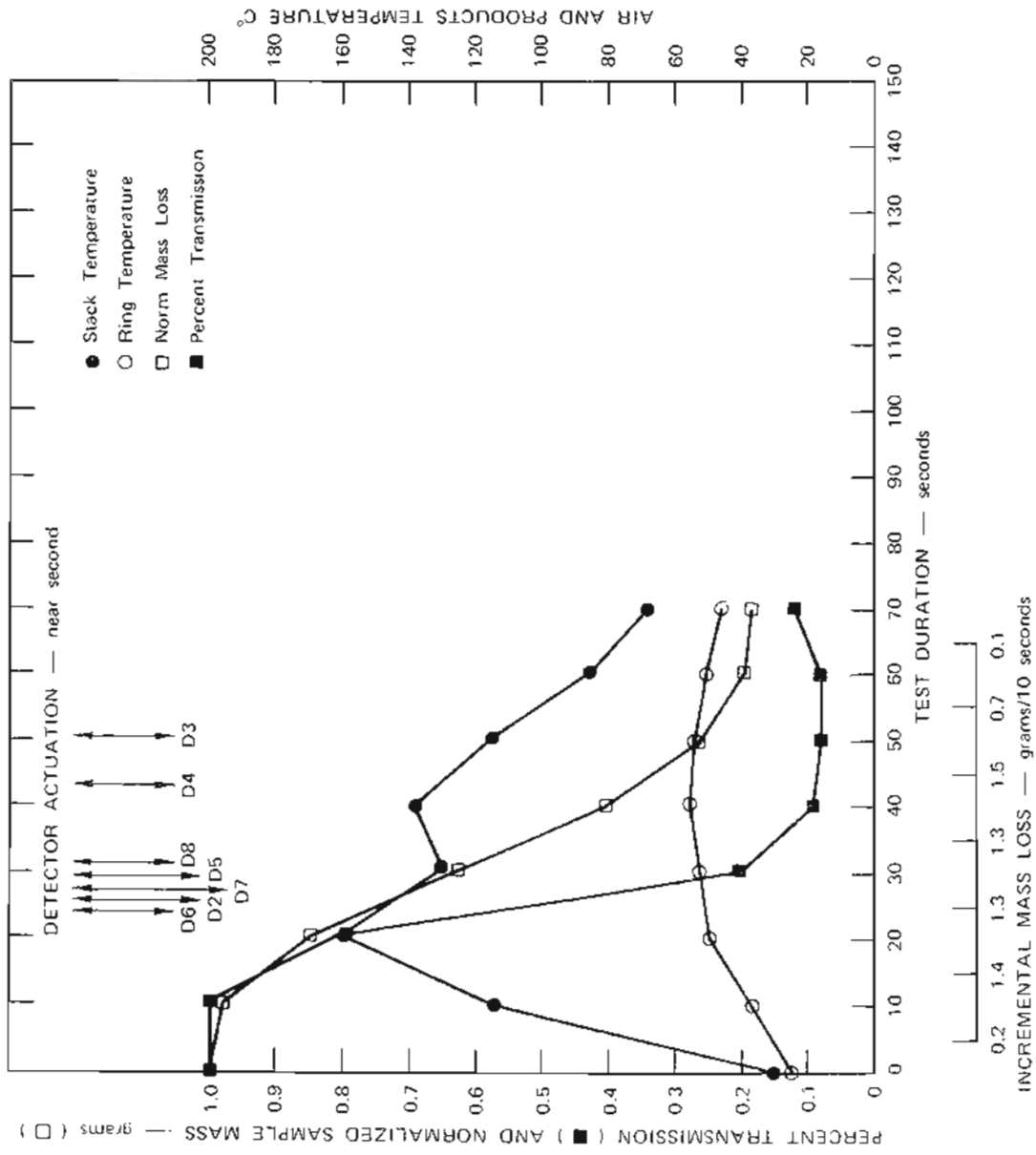
SA-3830-9

FIGURE 8 TEST 57—REPRODUCTION OF OSCILLOGRAPH RECORD



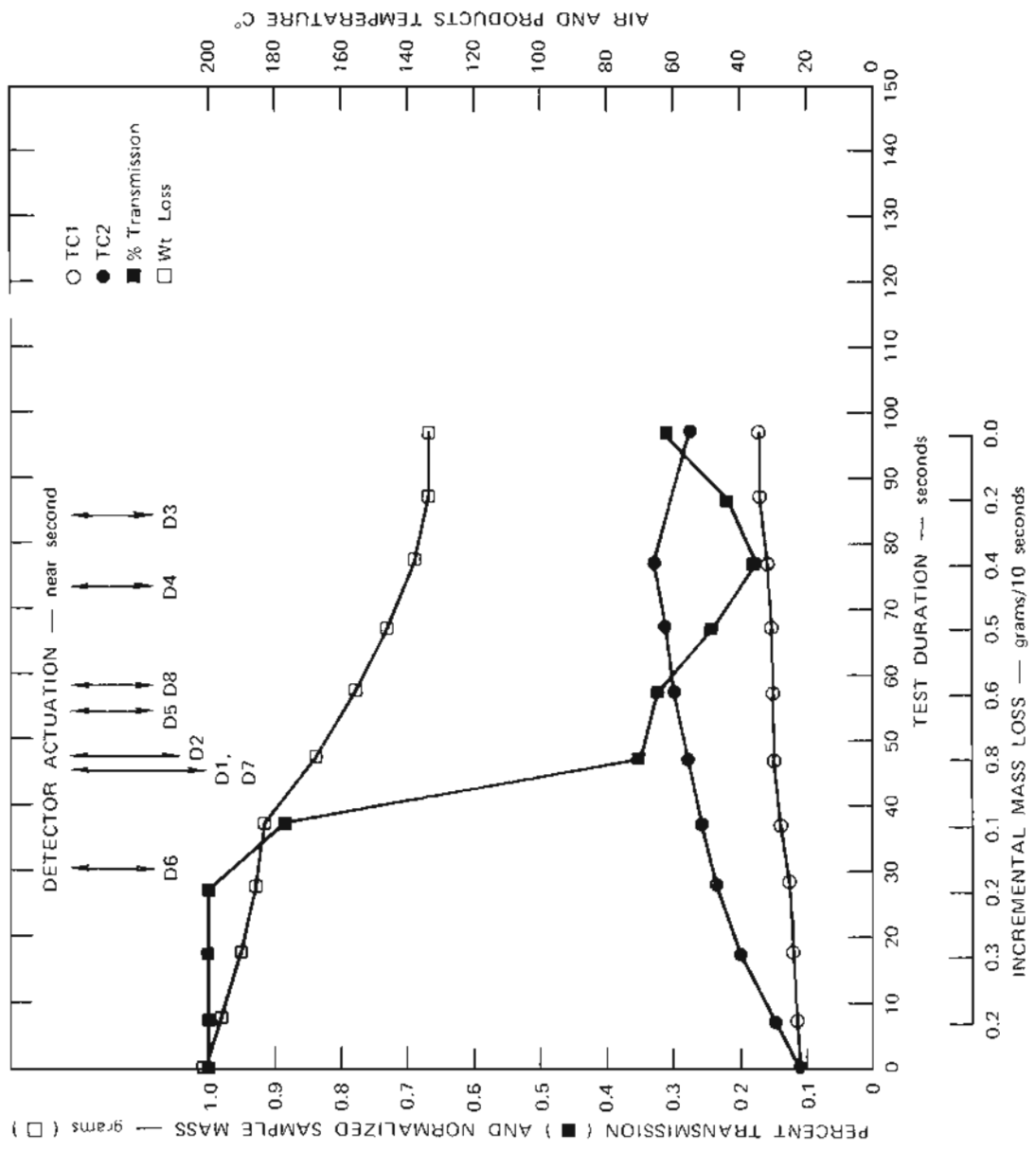
SA-3830-5

FIGURE 9 TEST 57—POLYESTER GLASS LAMINATE



SA-3830-11

FIGURE 10 TEST 106—POLYESTER GLASS LAMINATE



SA-3830-12

FIGURE 11 TEST 195—EPOXY GLASS FACES, NOMEX CORE

flame exposures because the thermal level is greater. This is apparent when the rate of smoke obscuration and detector response are compared in Figures 9 and 10.

Figure 11 shows the typical response of a fire-retarded composite material. The release of smoke from the composite is not apparent until some critical temperature or thermal level is reached. Beyond this level, the material expels smoke and loses weight at an accelerated rate.

In Figures 9 through 11 directly under the time scale for the test duration is a row of data that differentiate the incremental 10 sec mass loss during the detector alarm period. In Figure 9 both the time of material ignition ( $t_f$ ) and the power-off time for the radiant heat source are identified on the time scale. Across the top of the figure are the detector actuation identifiers. The near-second alarm time and the relationship of detector alarm to optical transmission, mass loss, and temperature variation also are shown.

The behavior of the optical transmission curves in Figures 9 and 11 are typical for the radiant exposure tests; if the material ignites, most of the volatile components have been pyrolyzed. Furthermore, after the source is shut off, the generation of airborne effluent is drastically reduced.

Table 3 summarizes the activation times for detectors exposed to the calibration polyurethane foam for the first series of radiant heat exposure tests. These data are derived from nine exposures that included both preliminary instrumentation tests and daily calibration tests. For Tests 2, 3, 25, and 43, the detectors were moved  $180^\circ$  from their normal position. This change of position combined with measurements of ceiling air velocities was made to determine if any asymmetry existed in the

Table 3

DETECTOR ACTUATION SUMMARY  
 [Times to Actuation (Sec) of Calibration  
 Polyurethane Foam, 0.048 g/cm<sup>3</sup>]

	D1 Gas Cell	D2 Pyrotronics Guardion Ionization	D3 Pyrotecator Scatter	D4 ESL 724 Visible Scatter	D5 ESL 824 Infrared Scatter	D6 Cerberus FM6 Ionization	D7 Cerberus RM6 Scatter	H	MAXOD	$\bar{m}$ $\Delta = 10$ sec	$t_F$
Test 1	61	38	113	60	42	44	21	1.1	0.824	1.43	61
Test 2 (180)	51	36	123	68	19	28	18	1.1	0.456	1.14	54
Test 3 (180)	45.5	36	112	56	28	33	21	1.1	0.481	1.40	48
Test 4	88	44	131	60	22	47	22	1.1	0.495	1.07	94
Test 5	58	37	57	90	17	28	23	1.1	0.638	1.21	124
Test 6	35	32	123	67	18.7	27.	33	0.8	0.638	1.63	48
Test 25 (180)	30	40	66	83	FA	26	19	0.8	0.602	0.94	No
Test 26	53	39	No	79	FA	36	33	0.8	0.769	1.33	67
Test 42	83	59	90	67	FA	51	27	0.8	0.553	1.2	52
Test 43 (180)	40	36	No	72	32	29	34	1.1	0.958	1.55	61
$t_r(\min)$	30	32	57	60	19	26	18		0.958	0.94	48
$t_r(\max)$	88	59	131	83	42	51	34		0.456	1.63	124
$t_r(\text{ave})$	54.5	39.7	101.9	70.2	24.5	34.9	25.1		0.638	1.29	60.9
$S_x$	19	7.5	27.8	10.9	9.4	9.2	6.2		8.0	21.7	25.4

Heading and symbol nomenclature:

H Irradiance in units of cal cm<sup>-2</sup> sec<sup>-1</sup>.

MAXOD Maximum optical density.

$\bar{m}$  Average mass loss of foam per 10-second period over the detector activation duration.

$t_F$  Time to flaming combustion.

(180) For tests 2, 3, 25, and 43, the detectors were moved 180° from the positions occupied during

tests 1, 4, 5, 6, 26, and 42.

$t_r$  Time and duration from radiant panel to flaming ignition of foam (min, max, ave indicate minimum, maximum,

and average times, respectively).

$S_x$  Standard deviation.

FA Instrument malfunction.

No No detection or detector activation.

system. The randomness of the data and the uniformity of the airflow at the ceiling confirm that there is no discernible asymmetry.

The actuation times in Table 3 are compared with the irradiance, the maximum optical density,<sup>\*</sup> the average weight loss rate as a function of alarm time, and the time-to-flaming ignition. Also included are the minimum, maximum, and average actuation times, pertinent test parameters, and the standard deviations of the response-time data.

The quantity of tests done with the calibration polyurethane foam permitted a simple statistical analysis of these data. By computing the standard deviation of the set of detector response data, we can appraise the dispersion of the individual detector response times to the pyrolysis products. The dispersion is probably a more valid measure of detector precision than is the relative time of actuation between detectors because the sensitivity of the detectors is set to prescribed levels of optical density or gas concentration during fabrication. Since sensitivity and false alarm frequency usually are inversely related, practical experience dictates the optimal setting for the different detectors. Consequently, if an instrument is relatively slow in response to the smoke from a particular material, we can assume that the detection cell labyrinth is long or tortuous and/or the sensitivity setting is low. If the detector's repeatability is high, however, the precision of the instrument is not compromised; rather, it may be a more reliable detector than one that usually actuates early during the exposure, but that lacks good repeatability.

#### Radiant Heat Exposure of Group I Materials

Table 4 summarizes the test parameters and detector response times for the set of detectors to the pyrolysis products from the first group of tested materials which were exposed to radiant heat.

---

\* Optical density =  $OD = \log_{10}(T)^{-1}$  where T is optical (visible light) transmittance expressed in percent over a 30.5-cm (1 ft) path length.



The response time data are presented in terms of the average, maximum, and minimum actuation times for three or more replications.\* Empty spaces in the columns indicate that the detector was unresponsive to the pyrolysis products in that test. Only the two ionization detectors responded to all materials. In general, the photoelectric detectors responded to everything except the products from light cellulosic material, whereas the gas sensor was sensitive to only four of the materials. Each detector that did not respond was checked with tobacco smoke after the failure. This procedure always succeeded in tripping the alarm circuits. In addition, the gas cell generally was triggered by vapors from solvents used to clean the test chamber.

The color of the material and the rate of radiant exposure are somewhat interdependent because the optical properties of the material partially control the fraction of energy absorbed. The thermal constants, thickness, and density determine how fast the material heats up; for example, black polyurethane foam requires much less energy to pyrolyze than does Lexan, which is a water-clear solid. Regardless of the higher irradiance ( $2.15 \text{ cal cm}^{-2} \text{ sec}^{-1}$ ), the heat-up time for the Lexan is still far longer than that for the foam, as reflected by the actuation times of the detectors.

The order in which the detectors actuated for each Group I material is shown in Table 5, along with the average actuation time and the average optical density at detector actuation. If the detector actuated

---

\* This number of tests provided insufficient data to compute a standard deviation for each detector. Hence, standard deviations are given only for the calibration foam.

Table 5

GROUP I. RADIANT HEAT EXPOSURE:  
ORDER OF DETECTOR ACTUATION

Material	First	Second	Third	Fourth	Fifth	Sixth	Seventh	$t_F^b$	MAXOD <sup>†</sup> MAXOD
Flexible polyurethane foam, 0.048 g/cm <sup>3</sup>	D5 24.5 <sup>‡</sup> 0.119	D7 25 0.125	D6 35 0.328	D2 39.7 0.357	D1 54.5 0.553	D4 70 MAXOD	D3 102 MAXOD	61	0.616 60
	D6 26.1 0.125	D7 26.8 0.125	D2 36 0.187	D3 80.6 MAXOD	D4 89 MAXOD			No	0.380 70
Flexible polyethylene foam, 0.032 g/cm <sup>3</sup>	D6 41 0.073	D7 48 0.149	D2 50.7 0.174	D4 86 MAXOD				47	0.194 60
	D5 49.5 0.015	D7 55 0.076	D6 64.4 0.058	D2 82.7 MAXOD	D6 97.5 MAXOD			74	0.131 78
Polyethylene film	D5 25.2 0.004	D6 37.4 0.007	D2 51 0.009	D7 74 0.099	D4 111.4 MAXOD			79.5	0.108 80
	D6 34.8 0.076	D7 37.4 0.099	D2 39.5 0.125	D3 83.6 0.530	D4 98.2 MAXOD			No	0.629 90
Molded ABS	D6 62.4 0.007	D2 81 0.013	D7 107 0.032	D4 137.3 MAXOD	D1 138.8 MAXOD	D3 151 MAXOD		115	0.602 130
	D7 32.9 0.114	D6 39 0.222	D5 40 0.250	D1 40.2 0.256	D2 49.4 0.420	D4 86.6 MAXOD	D3 96.3 MAXOD	54.5	0.745 58
Polyester-glass laminate	D6 54 0.007	D7 76 0.015	D2 77.2 0.056	D5 82.6 0.086	D4 114.4 0.342	D3 140 MAXOD		No	0.426 120
	D7 55.2 0.015	D5 64.3 0.026	D2 70.3 0.030	D6 71 0.033	D4 106.4 0.211	D3 147.2 MAXOD		No	0.333 123.5
Molded polystyrene	D2 77.7 MAXOD	D6 83.4 MAXOD	D5 87.1 MAXOD					68.6	0.025 80
	D6 81.6 MAXOD	D2 83.3 MAXOD	D5 83.3 MAXOD					74	0.013 75
100% Cotton fabric	D6 70.3 MAXOD	D7 72.6 MAXOD	D5 75.6 MAXOD	D2 82.0 MAXOD				65.6	0.013 70
	D6 73.5 MAXOD	D2 80.5 MAXOD	D5 87.1 MAXOD	D7 111.0 MAXOD				56.3	0.013 60
50% cotton/50% rayon fabric	D7 36.6 0.111	D6 38.7 0.131	D2 42.5 0.171	D3 47.0 0.478	D4 81.7 0.496			No	0.523 90
	D6 32.3 0.086	D7 36.6 0.102	D2 38.0 0.149	D3 48.0 0.432	D4 85.7 0.545			No	0.552 90
Paper towels	D6 33.0 0.018	D2 39.7 0.051	D7 44 0.180	D1 70.7 0.699	D4 85.7 0.824			No	0.824 87
Kleenex									
100% Wool fabric									
100% Wool carpet-latex back									
100% modacrylic carpet-latex back									

\* Average time to flame (sec).

† MAXOD =  $\frac{\text{maximum optical density}}{\text{time to maximum optical density}}$ ‡ D5 24.5 = designated detector  $\frac{\text{average actuation time (sec)}}{\text{optical density at average actuation time}}$ 

§ No means no flaming ignition.

after maximum optical density (MAXOD) was achieved, the abbreviation MAXOD is used in place of the numerical value for optical density. The time-to-flaming ignition, MAXOD, and the time-to-MAXOD are repeated from Table 4 to facilitate comparison with the detector response characteristics. The data in Table 5 yield the following observations:

- No detectors responded to pyrolysis products from cellulosic fuels until the material ignited.
- Ionization detectors usually actuated before photoelectric detectors.
- The detectors that were last to actuate usually triggered well after MAXOD. This was probably due to the impedance to smoke concentration buildup in the sensing chamber of the detector.
- The time delay to first detector actuation is more likely a characteristic of the material than of the detector and probably reflects differences in the absorption of radiant heat by the material rather than differences in composition.

Figure 12 contains a collection of averaged smoke transmission curves for a variety of material and illustrates the last point regarding time delay to first detector actuation. These curves show the effect of radiant energy absorption and thermal response of the material on the smoke production rate and the eventual detector actuation. For example, the materials that exhibit the earliest evidence of smoke production also indicate the earliest first detector actuation times. Materials that effectively reflect or transmit the exposure radiation have significantly longer first detector response times. However, the optical transmission of the smoke of the latter class of materials at detector actuation is significantly higher than the actuation optical transmission for the good absorbers.

Heskestad's<sup>1</sup> relationship between outer and inner detection chamber product concentrations may give insight into the role of detector flow

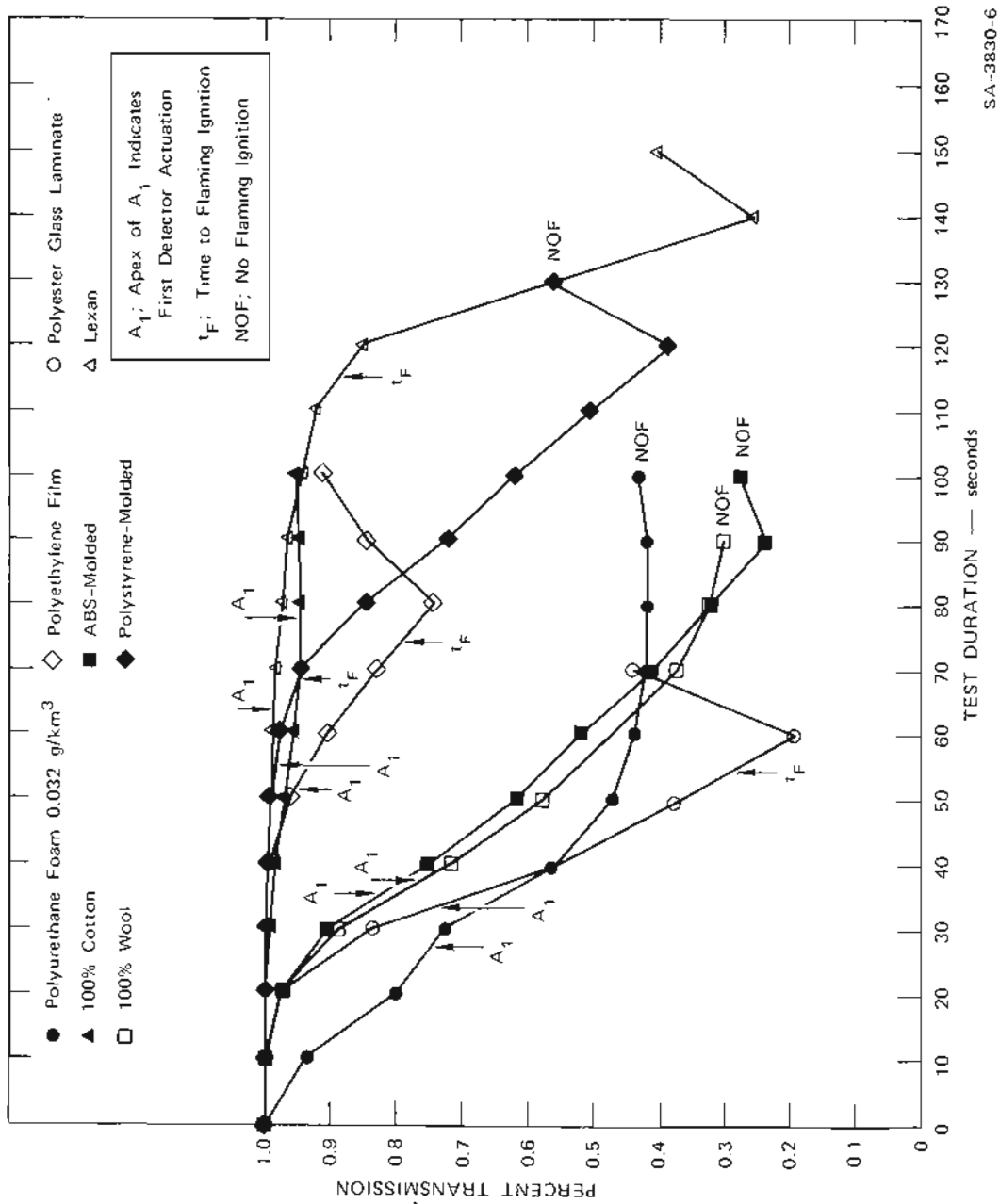


FIGURE 12 COMPOSITE AVERAGED OPTICAL TRANSMISSION FOR VARIOUS GROUP I MATERIALS TESTED

SA-3830-6

Table 6

GROUP I RADIANT HEAT EXPOSURE:  
OPTICAL DENSITY AT DETECTOR ACTUATION

Material	Average Optical Density at which Detector Activated							
	D1	D2	D3	D4	D5*	D6	D7	MAXOD†
Flexible polyurethane foam, .048 g/cm <sup>3</sup>	0.553	0.357	PMOD‡	PMOD	0.119	0.328	0.125	0.616
Flexible polyurethane foam, .032 g/cm <sup>3</sup>		0.187	PMOD	PMOD	FA	0.125	0.125	0.380
Flexible polyethylene foam, .032 g/cm <sup>3</sup>		0.174		PMOD	FA	0.073	0.149	0.194
Polyethylene film		PMOD		PMOD	0.015	0.058	0.026	0.131
Molded polyethylene		0.009		PMOD	0.004	0.007	0.099	0.108
Molded ABS		0.125	0.530	PMOD	FA	0.076	0.099	0.629
Lexan	PMOD	0.013	PMOD	PMOD	FA	0.007	0.032	0.602
Polyester-glass laminate	0.256	0.420	PMOD	PMOD	0.250	0.220	0.114	0.745
Molded polystyrene		0.056	PMOD	0.342	0.086	0.007	0.015	0.426
Styrofoam cups		0.030	PMOD	0.211	0.026	0.033	0.015	0.333
100% Cotton fabric		PMOD			FA	PMOD		0.025
50% Cotton/50% rayon fabric		PMOD			FA	PMOD		0.013
Paper towels		PMOD			PMOD	PMOD	PMOD	0.013
Kleenex		PMOD			PMOD	PMOD	PMOD	0.013
100% Wool Fabric		0.171	0.478	0.494	FA	0.131	0.111	0.523
100% Wool carpet-latex back		0.149	0.432	0.545	FA	0.086	0.102	0.553
100% Modacrylic carpet-latex back	0.699	0.051	PMOD	0.824	FA	0.018	0.051	0.824

\* FA indicates false alarming. Detector D5 was initially functioning, but became erratic and was replaced roughly halfway through the test series.

† MAXOD = maximum optical density.

‡ PMOD = detector actuates past the time of maximum optical density (for those materials that ignite, PMOD implies past ignition time also).

pertaining to the smoke production dynamics of the flame-exposed material. Table 7 summarizes the results of this survey. The only interesting results from this table are derived from comparison of the burning rate data with the detector response data contained in Table 8. In general, materials with high burning rates would be expected to produce voluminous combustion products that would result in quick alarm response from the detectors, and the reverse response would be expected from slow burners or those materials that do not self-sustain combustion. To the contrary, the data in Tables 7 and 8 indicate that such generalizations would be unwise because the response of detectors to the various combustion products is independent of the burning rate.

Comparison of Tables 8 and 9 with Tables 5 and 6 (order of detector activation and optical density at detector activation) yields no unusual inconsistencies, however, all detectors generally respond approximately 20% faster during the flame exposures. This increased response could result from either the greater combustion product generation or the enhanced convection potential of the flame source--that is the air velocities are approximately 10% faster for the flame exposure in the region of the detector ring. The data trends are similar for both the radiant heat panel and flame exposure tests. Thus, detectors D2, D5, D6 and D7 all compete for first through third place in terms of detector actuation times. The optical density at the time of detector actuation appears to be slightly less than in the radiant heat exposure tests for all detectors for some materials and more for others, (notably larger for polyester- and polystyrene-based materials and less for polyurethane- and polyethylene-based materials). Comparison of the maximum, minimum, and average values of optical densities from flame and smoldering

Table 7

## GROUP I MATERIALS: PRELIMINARY FLAME TESTS

Material	Average Burning Rate* (g/min)	Self-Sustaining Flame <sup>†</sup>
Polyurethane foam, 0.048 g/cm <sup>3</sup>	5.17	Yes
100% Wool fabric	2.07	No
100% Cotton fabric	3.35	Yes
50% Cotton/50% Rayon fabric	3.36	Yes
Paper towel	2.31	Yes
Polyethylene film	1.36	Yes
Polyethylene foam	1.55	Yes
Polyurethane foam, 0.032 g/cm <sup>3</sup>	2.72	No <sup>‡</sup>
100% Wool carpet with latex backing	1.31	No <sup>δ</sup>
Modacrylic carpet with latex backing	1.93	No <sup>δ</sup>
Polyethylene cast	0.94	Yes
Polystyrene cast	1.00	Yes
Lexan	0.66	No
ABS	1.52	Yes
Styrofoam cups	2.01	No
Fire-retardant polyurethane foam	1.30	No

\* Initial sample weight approximately 10 g.

<sup>†</sup> Sample maintained flame without aid of Meeker burner.

<sup>‡</sup> Flame self-sustaining when sample melted.

<sup>δ</sup> Sample will self-sustain when flame reaches backing.

Table 8

GROUP I FLAME EXPOSURE  
AND GROUP II HEATED COIL EXPOSURE  
ORDER OF DETECTOR ACTUATION

Material	First	Second	Third	Fourth	Fifth	Sixth	Seventh	Eighth	$\frac{\text{MAXOD}^\dagger}{\text{tMAXOD}}$
Group I - Flame									
Polyurethane foam, 0.048 g/cm <sup>3</sup>	D6 $\frac{19.8^*}{0.115}$	D7 $\frac{21.4}{0.119}$	D2 $\frac{22.2}{0.122}$	D5 $\frac{28.75}{0.143}$	D4 $\frac{59.6}{0.141}$	D3 $\frac{59.6}{0.141}$	-	-	$\frac{0.167}{40}$
Polyurethane foam, 0.032 g/cm <sup>3</sup>	D2 $\frac{11.27}{0.032}$	D7 $\frac{15.67}{0.058}$	D6 $\frac{16.17}{0.063}$	D5 $\frac{18.33}{0.078}$	D4 $\frac{31.23}{0.149}$	D3 $\frac{56.0}{0.237}$	D8 $\frac{56.2}{0.240}$	-	$\frac{0.267}{70}$
Polyethylene foam 0.032 g/cm <sup>3</sup>	D6 $\frac{47.1}{0.004}$	D3 $\frac{48.13}{0.004}$	D7 $\frac{98.9}{0.024}$	D5 $\frac{109.3}{0.038}$	D4 $\frac{155.3}{0.140}$	-	-	-	$\frac{0.208}{180}$
Styrofoam cups	D7 $\frac{16.4}{0.240}$	D2 $\frac{17.73}{0.264}$	D5 $\frac{17.97}{0.284}$	D6 $\frac{21.67}{0.342}$	D8 $\frac{47.83}{0.509}$	D4 $\frac{60.17}{0.602}$	D3 $\frac{84.6}{0.730}$	-	$\frac{1.0}{120}$
100% Wool carpet	D2 $\frac{22.87}{0.001}$	D6 $\frac{26.4}{0.001}$	D6 $\frac{194.2}{0.032}$	D7 $\frac{214.8}{0.038}$	D4 $\frac{219.5}{0.041}$	-	-	-	$\frac{0.056}{260}$
Polyester-glass laminate	D6 $\frac{26.6}{0.319}$	D6 $\frac{29.47}{0.482}$	D7 $\frac{29.5}{0.488}$	D2 $\frac{30.03}{0.523}$	D8 $\frac{34.8}{0.664}$	D3 $\frac{50.1}{0.980}$	D4 $\frac{53.67}{\text{PMOD}}$	-	$\frac{0.980}{50}$
50% Cotton/50% rayon fabric	D2 $\frac{48.9}{0.001}$	D6 $\frac{62.0}{0.004}$	-	-	-	-	-	-	$\frac{0.004}{65}$
100% Cotton fabric	D2 $\frac{42.0}{0.001}$	D6 $\frac{48.5}{0.004}$	-	-	-	-	-	-	$\frac{0.004}{50}$
Paper towel	D2 $\frac{39.8}{0.001}$	D6 $\frac{48.5}{0.001}$	-	-	-	-	-	-	$\frac{0.01}{70}$
Kleenex	D2 $\frac{61.0}{0.004}$	D6 $\frac{61.0}{0.004}$	-	-	-	-	-	-	$\frac{0.004}{65}$
Polyethylene film	D2 $\frac{51.77}{0.001}$	D6 $\frac{90.4}{0.004}$	D7 $\frac{149.7}{0.071}$	D5 $\frac{154.7}{0.080}$	D4 $\frac{213.5}{0.177}$	D3 $\frac{232.0}{\text{PMOD}}$	-	-	$\frac{0.225}{320}$
100% Wool fabric	D2 $\frac{20.9}{0.001}$	D6 $\frac{28.2}{0.001}$	-	-	-	-	-	-	$\frac{0.004}{80}$
Modacrylic carpet	D6 $\frac{25.1}{0.012}$	D2 $\frac{25.3}{0.012}$	D5 $\frac{52.3}{0.015}$	D7 $\frac{136.4}{\text{PMOD}}$	-	-	-	-	$\frac{0.021}{53.3}$
Lexan	D6 $\frac{97.5}{0.013}$	D2 $\frac{102.7}{0.011}$	D5 $\frac{107.9}{0.014}$	D7 $\frac{152.8}{0.044}$	D3 $\frac{178.0}{0.069}$	D4 $\frac{196.0}{0.127}$	-	-	$\frac{0.175}{206.6}$
Polyethylene cast	D6 $\frac{115.4}{0.006}$	D2 $\frac{120.0}{0.007}$	D7 $\frac{208.2}{0.018}$	D5 $\frac{373.5}{\text{PMOD}}$	D4 $\frac{383.0}{\text{PMOD}}$	-	-	-	$\frac{0.026}{366.6}$
Polystyrene	D6 $\frac{38.4}{0.063}$	D2 $\frac{38.7}{0.063}$	D5 $\frac{10.5}{0.067}$	D7 $\frac{46.0}{0.079}$	D8 $\frac{111.5}{0.456}$	D4 $\frac{124.5}{0.580}$	D3 $\frac{131.4}{0.630}$	-	$\frac{0.886}{136.6}$
Fire retardant polyurethane foam	D2 $\frac{19.3}{0.083}$	D7 $\frac{19.6}{0.088}$	D6 $\frac{19.8}{0.088}$	D5 $\frac{23.7}{0.127}$	D8 $\frac{40.5^{\ddagger}}{0.168}$	D4 $\frac{48.5}{0.159}$	D3 $\frac{72.2}{\text{PMOD}}$	-	$\frac{0.178}{53.3}$
Neoprene with cord filler	D2 $\frac{31.3}{0.019}$	D6 $\frac{33.9}{0.020}$	D7 $\frac{57.6}{0.031}$	D5 $\frac{59.6}{0.032}$	D4 $\frac{81.4}{0.160}$	D3 $\frac{129.5}{\text{PMOD}}$	-	-	$\frac{0.296}{109.6}$
ABS, molded	D6 $\frac{28.9}{0.021}$	D2 $\frac{43.6}{0.077}$	D7 $\frac{63.0}{0.178}$	D5 $\frac{72.0}{0.219}$	D8 $\frac{111.2}{0.432}$	D3 $\frac{114.5}{0.465}$	D4 $\frac{128.4}{0.474}$	-	$\frac{0.490}{126.6}$
Group II - Smoldering									
100% Cotton fabric	D2 $\frac{170.6}{0.028}$	D5 $\frac{173.1}{0.031}$	D6 $\frac{183.3}{0.037}$	D7 $\frac{183.8}{0.037}$	D1 $\frac{286}{0.123}$	D3 $\frac{338}{\text{PMOD}}$	-	-	$\frac{0.142}{320}$
50% Rayon/50% cotton fabric	D5 $\frac{147.7}{0.024}$	D2 $\frac{162.4}{0.035}$	D7 $\frac{165.6}{0.037}$	D6 $\frac{177.4}{0.044}$	D4 $\frac{264.7}{\text{PMOD}}$	D3 $\frac{307.2}{\text{PMOD}}$	-	-	$\frac{0.106}{260}$
Paper towel	D5 $\frac{232.7}{0.025}$	D6 $\frac{244}{0.027}$	D7 $\frac{246.3}{0.029}$	D2 $\frac{246.6}{0.029}$	D4 $\frac{441.1}{\text{PMOD}}$	-	-	-	$\frac{0.072}{100}$
Kleenex	D5 $\frac{184.3}{0.024}$	D7 $\frac{219.9}{0.36}$	D6 $\frac{233}{0.041}$	D2 $\frac{233.7}{0.041}$	-	-	-	-	$\frac{0.109}{320}$

\* D6  $\frac{19.8}{0.115}$  = detector designation average alarm time (sec)  
optical density at alarm

†  $\frac{\text{MAXOD}}{\text{tMAXOD}}$  =  $\frac{\text{maximum optical density}}{\text{time to maximum optical density}}$  ; PMOD denotes post maximum optical density.

‡ Alarm on one of three tests

Table 9

GROUP I FLAME EXPOSURE AND GROUP II HEATED COIL EXPOSURE:  
OPTICAL DENSITY AT DETECTOR ACTUATION

Material	Average Optical Density at which Detector Activated								MAXOD*
	D1	D2	D3	D4	D5	D6	D7	D8	
	<u>Group I - Flame</u>								
Polyurethane <sub>3</sub> foam, 0.048 g/cm <sup>3</sup>		0.122	0.141	0.143	0.143	0.115	0.119		0.167
Polyurethane <sub>3</sub> foam, 0.032 g/cm <sup>3</sup>		0.032	0.237	0.149	0.078	0.06	0.058	0.240	0.267
Polyethylene foam		0.004		0.140	0.036	0.004	0.024		0.208
Styrofoam cups		0.264	0.730	0.602	0.284	0.342	0.240	0.509	1.000
100% Wool with latex backing (carpet)		0.001		0.041	0.032	0.001	0.038		0.056
Polyester glass laminate		0.523	MAXOD	PMOD <sup>†</sup>	0.482	0.319	0.488	0.664	0.980
50% Cotton/50% rayon fabric		0.001				0.001			0.004
100% Cotton fabric		0.001				0.004			0.004
Paper towel		0.001				0.001			0.010
Kleenex		0.004				0.004			0.004
Polyethylene film		0.001	PMOD	0.177	0.080	0.004	0.071		0.225
100% Wool fabric		0.001				0.001			0.004
Modacrylic (carpet)		0.012			0.015	0.012	PMOD		0.021
Lexan		0.011	0.069	0.127	0.014	0.013	0.044		0.175
Polyethylene cast		0.007		PMOD	PMOD	0.006	0.018		0.026
Polystyrene cast		0.063	0.630	0.580	0.067	0.063	0.079	0.456	0.886
Fire-retardant Poly- urethane foam		0.083	PMOD	0.159	0.127	0.088	0.088	0.168	0.178
Neoprene with cord filler ABS (molded)		0.077	0.465	0.474	0.219	0.021	0.178	0.432 <sup>‡</sup>	0.490
	<u>Group II - Smoldering</u>								
100% Cotton fabric	0.123	0.028	PMOD		0.031	0.037	0.037		0.142
50% Cotton/50% rayon fabric		0.035	PMOD	PMOD	0.024	0.044	0.037		0.106
Paper towel		0.029		PMOD	0.025	0.027	0.029		0.072
Kleenex		0.011			0.024	0.041	0.036		0.019

\* MAXOD - denotes maximum optical density.

† PMOD - denotes past maximum optical density.

‡ Alarm on one of three tests.

exposure at detector activation for the photoelectric detectors as shown below indicates a slight increase in all values relative to the radiant heat exposure data previously listed.

<u>Detector</u>	<u>Average</u>	<u>Maximum</u>	<u>Minimum</u>
D3	0.395	0.980	0.069
D4	0.289	0.980	0.26
D5	0.118	0.482	0.014
D6	0.107	0.488	0.018

This behavior undoubtedly is attributable to the different mechanisms of smoke formation during pyrolysis and flaming combustion. An interesting corollary in this respect is the comparison of the responses of the photoelectric detectors between the smoke from radiant heat exposure with that from flame exposures of 100% wool fabric. In both cases, the fabric does not burn, but apparently the flame source either brings about removal of the aerosol responsible for photoelectric activation or possibly changes the aerosol size distribution to the extent that the particulates do not provide efficient scattering densities.

#### Heated Coil Exposure of Group II Materials

During the tests that exposed the detectors to the products from smoldering cellulosic fuels, all of the more reliable detectors responded at essentially the same time and optical density. Note in Table 9 that the gas sensor (detector D1) did respond (one time only) to the smoldering products from 100% cotton fabric.

#### Radiant Heat Exposure of Group III Materials

Tables 10 and 11 list the detector response characteristics for the Group III advanced fire-retardant materials exposed to the radiant heat

Table 10

GROUP 111 RADIANT HEAT EXPOSURE  
ORDER OF DETECTOR ACTUATION

Material	First	Second	Third	Fourth	Fifth	Sixth	Seventh	Eighth	Ninth	Tenth	tf	MAXOD†
Acrylonitrile butadiene styrene (ABS)	D9R 32.3	D6 35.3	D7 37.7	D5 38.4	D9L 38.6	D2 42.0	D1 42.6	D8 55.3	D4 79.3	D3 85.4	No	0.70
	0.143	0.157	0.240	0.240	0.260	0.292	0.298	0.393	0.611	0.620	No	107.0
Chlorinated polyvinyl chloride (PVC)	D9R 38.7	D6 43.0	D9L 48.2	D1 62.6	D2 64.1	D7 65.4	D5 83.5	D8 98.7	D4 99.8	-	No	0.150
	0.007	0.01	0.017	0.077	0.076	0.083	0.131	0.149	0.148	-	No	104.3
Polycarbonate	D9R 88.6	D6 72.7	D2 82.3	D9L 104.3	D7 172.3	D6 174.0	D4 201.4	D8 206.4	D1 236.5	D3 280.1	No	0.504
	0.001	0.001	0.001	0.001	0.041	0.047	0.128	0.134	0.197	PMOD	No	240
PBI fabric	D9R 49.9	D6 58.9	D7 60.0	D6 62.3	D2 65.1	D9L 76.0	D1 124.6	-	-	-	No	0.021
	0.0125	0.013	0.013	0.013	0.014	0.014	0.018	-	-	-	No	98.7
Kynol cloth	D1 55.5	D6 63.8	D9R 71.1	D2 73.9	D5 79.4	D9L 90.6	D7 100.6	-	-	-	84.7	0.019
	0.004	0.005	0.009	0.009	0.009	0.011	0.017	-	-	-	84.7	97.3
Polyether sulfone	D6 53.4	D2 80.6	D7 98.0	D9R 101.5	D5 104.3	D1 106.8	D8 119.2	D4 123.7	D9L 127.6	D3 225.3	152.0	0.309
	0.008	0.010	0.057	0.083	0.10	0.11	0.141	0.161	0.167	PMOD	158.0	158.0
New LS polycarbonate F-6000	D6 76.7	D2 96.1	D7 168.8	D5 172.9	D9R 188.0	D9L 202.3	D4 204.5	D8 214.4	D1 223.3	D3 299.0	No	0.353
	0.001	0.001	0.018	0.022	0.057	0.115	0.111	0.199	0.235	PMOD	No	234
Modified polyphenylene oxide (Noryl)	D6 40.3	D7 45.0	D1 45.2	D2 51.9	D5 59.1	D8 64.8	D9L 69.1	D4 78.7	D3 97.1	-	No	0.552
	0.123	0.210	0.210	0.339	0.419	0.406	0.510	0.586	PMOD	-	No	88
Betron	D6 36.2	D9R 44.8	D2 59.4	D5 60.1	D7 61.1	D9L 74.5	D1 78.1	D8 81.5	D4 91.2	D3 210.2	No	0.962
	0.004	0.013	0.037	0.041	0.041	0.114	0.141	0.167	0.252	PMOD	No	108
Modified polysulfone	D6 52.7	D9R 60.5	D2 89.2	D5 90.1	D7 98.0	D9L 104.7	D1 109.6	D4 128.9	D8 132.9	-	No	0.198
	0.001	0.001	0.023	0.026	0.036	0.057	0.077	0.138	0.153	-	No	146.3
Polyethylene sulfide	D6 50.1	D7 75.4	D5 80.1	D9R 88.6	D2 96.2	D4 108.4	D8 119.4	D9L 119.4	D1 120.2	D3 142.5	No	0.140
	0.009	0.024	0.035	0.043	0.053	0.075	0.093	0.093	0.095	PMOD	No	142.5
Komec fabric	D6 59.6	D2 79.3	D7 111.7	D5 122.4	D8 134.3	D4 139.8	D3 192.2	-	-	-	No	0.436
	0.001	0.001	0.052	0.151	0.264	0.331	PMOD	-	-	-	No	158.3
Silicone elastomer	D6 53.3	D2 89.0	D7 98.4	D4 142.2	D5 142.2	D8 185.0 <sup>‡</sup>	-	-	-	-	No	0.159
	0.001	0.001	0.003	0.086	0.056	PMOD	-	-	-	-	No	83.6
Epoxy glass face, Komec core	D6 32.8	D7 42.5	D1 43.8	D2 48.9	D8 45.8	D5 54.0	D4 81.3	D3 92.4	-	-	No	0.664
	0.048	0.290	0.356	0.464	0.458	0.458	PMOD	PMOD	-	-	No	76.0
Tedlar-coated phenolic glass faces, Komec core	D6 33.8	D2 36.4	D7 41.3	D1 46.5	D5 49.5	D8 58.9	D4 72.0	D3 84.3	-	-	No	0.558
	0.078	0.097	0.147	0.284	0.391	0.328	0.417	0.523	-	-	No	85.0
Tedlar-coated phenolic glass laminate	D5 31.0	D6 44.4	D2 48.9	D7 59.0	D1 69.2	D8 86.4	D4 98.4	D3 108.7	-	-	No	0.217
	0.001	0.033	0.031	0.092	0.127	0.194	0.198	0.201	-	-	No	103.3
Tedlar, PVC film	D6 22.5	D5 30.7	D7 37.4	D1 102.6	D2 107.1	D4 115.4	D8 126.3	D3 175.0	-	-	No	0.377
	0.001	0.001	0.059	0.084	0.130	0.143	0.244	PMOD	-	-	No	132.3
Fire-retardant polyurethane foam	D5 23.6	D7 24.0	D6 24.4	D2 26.1	D1 26.2	D4 88.3	D4 79.9	-	-	-	No	0.420
	0.292	0.314	0.317	0.377	0.367	PMOD	PMOD	-	-	-	No	50.0
Neoprene with cord filler	D2 39.6	D7 41.0	D6 42.4	D5 47.4	D8 56.0	D3 75.2	D1 107.5	-	-	-	No	0.855
	0.220	0.243	0.256	0.317	0.433	0.880	PMOD	-	-	-	No	93.3

<sup>‡</sup> 32.3 = average alarm time (sec)  
D9R 0.143 = detector designation  
optical density at alarm time  
† MAXOD = maximum optical density  
time to maximum optical density (sec)

<sup>‡</sup> D9 removed for remainder of materials  
‡ Alarm on one of three tests.

Table 11

 GROUP III RADIANT HEAT EXPOSURE:  
 OPTICAL DENSITY AT DETECTOR ACTUATION

Material	Average Optical Density at which Detector Activated										
	D1	D2	D3	D4	D5	D6	D7	D8	D9R	D9L	MAXOD
Acrylonitrile butadiene styrene (ABS)	0.298	0.292	0.620	0.611	0.240	0.157	0.240	0.393	0.143	0.260	0.700
Chlorinated polyvinyl chloride (PVC)	0.077	0.076		0.148	0.131	0.010	0.083	0.149	0.007	0.017	0.150
Polycarbonate	0.187*	0.001	PMOD†	0.128	0.0466	0.001	0.041	0.134	0.001	0.001	0.504
PBI fabric	0.018	0.014			0.013	0.013	0.013		0.012	0.014	0.021
Kynol cloth	0.004	0.009			0.009	0.005	0.017		0.009	0.011	0.019
Polyether sulfone	0.110	0.010		0.161	0.099	0.008	0.057	0.141	0.083	0.167	0.309
New LS polycarbonate F-6000	0.235‡	0.001	PMOD	0.111	0.022	0.001	0.018	0.199	0.057	0.115	0.353
Modified polyphenylene oxide (Noryl)	0.210	0.339	PMOD	0.586	0.419	0.123	0.210	0.406		0.510	0.632
Retron	0.141	0.037	PMOD	0.252	0.041	0.004	0.041	0.167	0.013	0.114	0.362
Modified polysulfone	0.077	0.023		0.138	0.026	0.001	0.036	0.153	0.001	0.057	0.198
Polyphenylene sulfide	0.095	0.053		0.075	0.035	0.009	0.024	0.093	0.043	0.093	0.140
Nomex fabric		0.001	PMOD	0.331	0.151	0.001	0.052	0.264	§	§	0.436
Silicone elastomer		0.001		0.056	0.056	0.001	0.003	PMOD			0.159
Epoxy glass face, Nomex core	0.356	0.464	PMOD	PMOD	0.458	0.048	0.290	0.458			0.664
Tedlar-coated phenolic glass faces, Nomex core	0.284	0.097	0.523	0.417	0.291	0.078	0.187	0.328			0.538
Tedlar-coated phenolic glass laminate	0.127	0.031	0.201	0.198	0.001	0.033	0.092	0.194			0.217
Tedlar PVC film	0.084	0.130	PMOD	0.143	0.001	0.001	0.059	0.244			0.377
Fire-retardant polyurethane foam	0.367	0.377	PMOD	PMOD	0.292	0.317	0.314				
Neoprene with cord filler		0.220	0.680	PMOD	0.317	0.256	0.243	0.433			

\* Alarm on one of three tests before MOD (maximum optical density).

† PMOD indicates alarm past maximum optical density.

‡ Alarm on three of four tests before MOD.

§ Removed for remainder of tests.

source. In addition to the photoelectric and ionization detectors used in the preceding test series, we included the special detector supplied by the Celesco Company and the replacement for the KF industries gas sensor (D1) which was damaged during the earlier flame exposure tests. The Celesco detector is a hybrid unit consisting of a Pyrotronic twin ionization chamber, using Americium 241 as the ionization source. The source is contained in a Celesco-designed package that includes a pumping system for classifying and flowing the aerosol through the ionization elements and electrical signal discriminating circuitry. The Celesco detector generates two alarms: a concentration (c) or level alarm and a rate alarm (dc/dt). Both of these alarms from the detector were recorded. In addition, using a Celesco-designed quartz crystal microbalance, Celesco personnel made measurements of the particle mass accumulation during the tests in which they participated.

The detectors which consistently and effectively responded to the pyrolysis products in the previous tests responded similarly in these tests with the Group III materials. The new replacement gas detector (D1) also gave a creditable performance during this test series, probably because of an improvement in its design. Detectors D2, D5, D6, and D7 responded in adequate time and at sufficiently modest optical densities to all of the tested materials. Detectors D1, D4, and D8 responded to all but three of the materials; and D3 followed its normal pattern. The Celesco instrument, D9, was comparable to the better responding photoelectric and ionization detectors; however, the pump portion of the detector experienced difficulties when the smoke load was high. On both units the particulates from the smoke gradually built up a deposit on the rotary vane to the point that the pump no longer would function.

The list below compares the relative response optical density data from Group III materials exposed to radiant heat for the photoelectric detectors.

<u>Detector</u>	<u>Average</u>	<u>Maximum</u>	<u>Minimum</u>
D3	0.477	0.680	0.201
D4	0.298	0.680	0.056
D5	0.139	0.458	0.001
D7	0.105	0.314	0.003
D8	0.244	0.458	0.093

Note that only D5 and D7 of the five photoelectric detectors alarmed to all exposures (see Table 11). The trend of these data is similar to that for the optical density response for both the radiant heat and flame exposure tests conducted with the more common Group I materials.

#### Air Velocity, Humidity, and Ambient Pressure Effects on Detector Performance

Time constraints disallowed a study of air velocity effects on the detectors tested during this program. The literature, however, offers considerable data concerning this problem. Recent tests were made by the Gillette Research Institute<sup>2</sup> to ascertain flow velocity effects on the alarm parameters of ionization and photoelectric detectors. The next two figures are from the Gillette report. Figure 13 shows the response of the ionization detector that is similar to detector D6 used in our tests. Figure 14 indicates the response for a photoelectric detector that is similar to the D5 used in our tests. Obviously, the ionization detector is highly sensitive to flow, whereas the photoelectric detector apparently has little sensitivity to flow. For all the exposure tests we conducted, the airflow rate at the detector ring

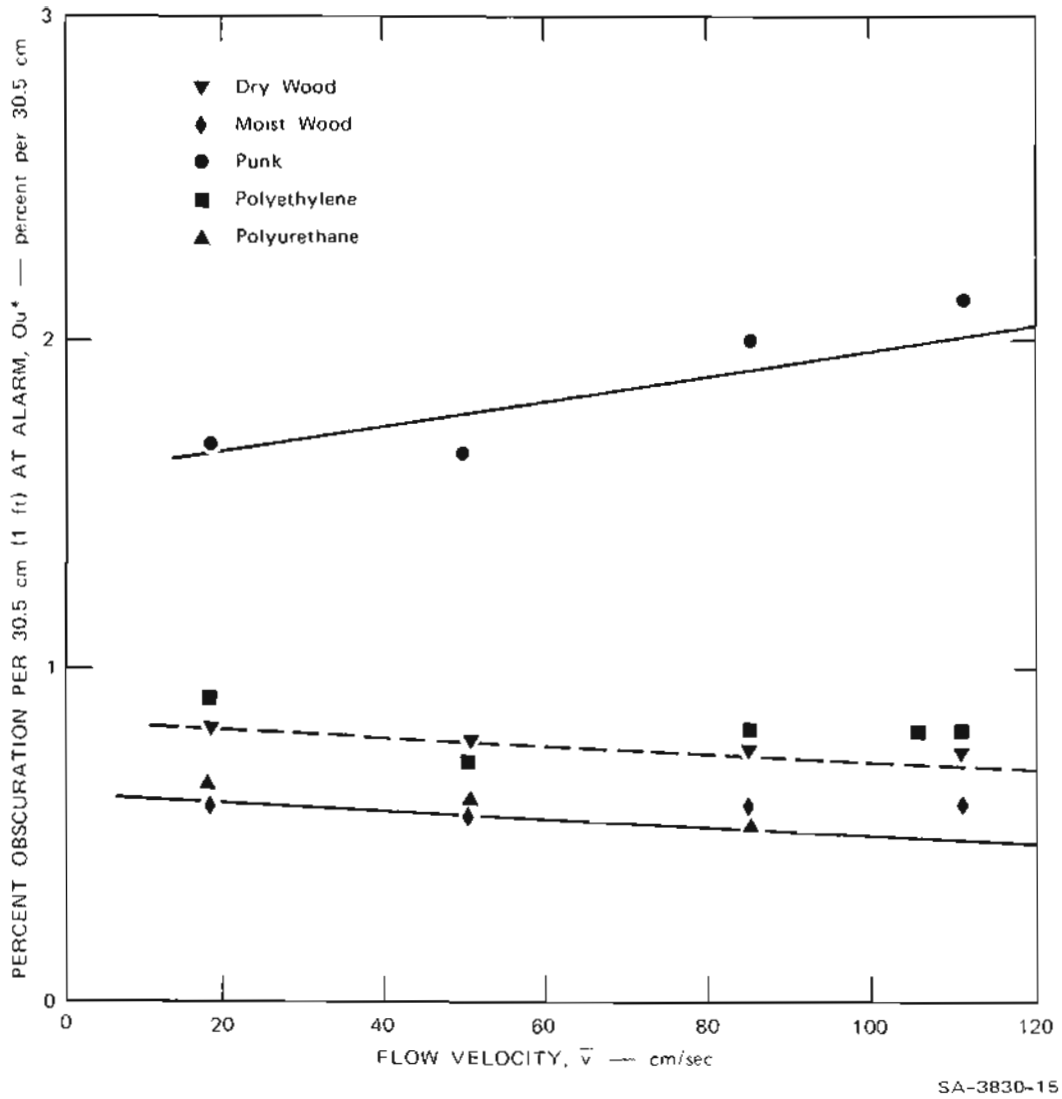


FIGURE 13 PLOT OF  $O_u^*$  VERSUS  $\bar{v}$  FOR PYROTECTOR SK 700 LED SMOKE DETECTOR

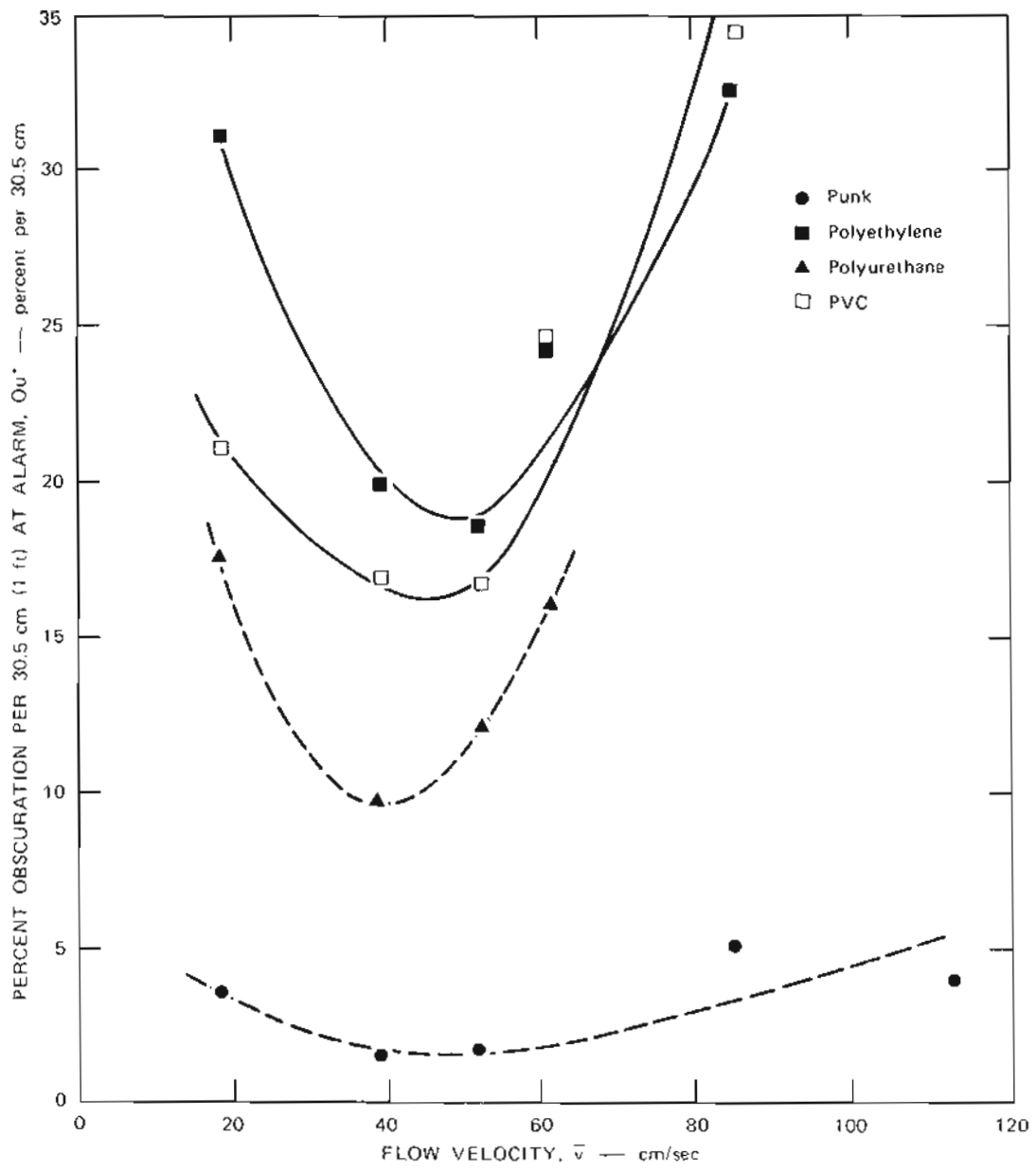


FIGURE 14 PLOT OF  $O_u^*$  VERSUS  $\bar{v}$  FOR PYR-A-LARM DI-2S IONIZATION DETECTOR

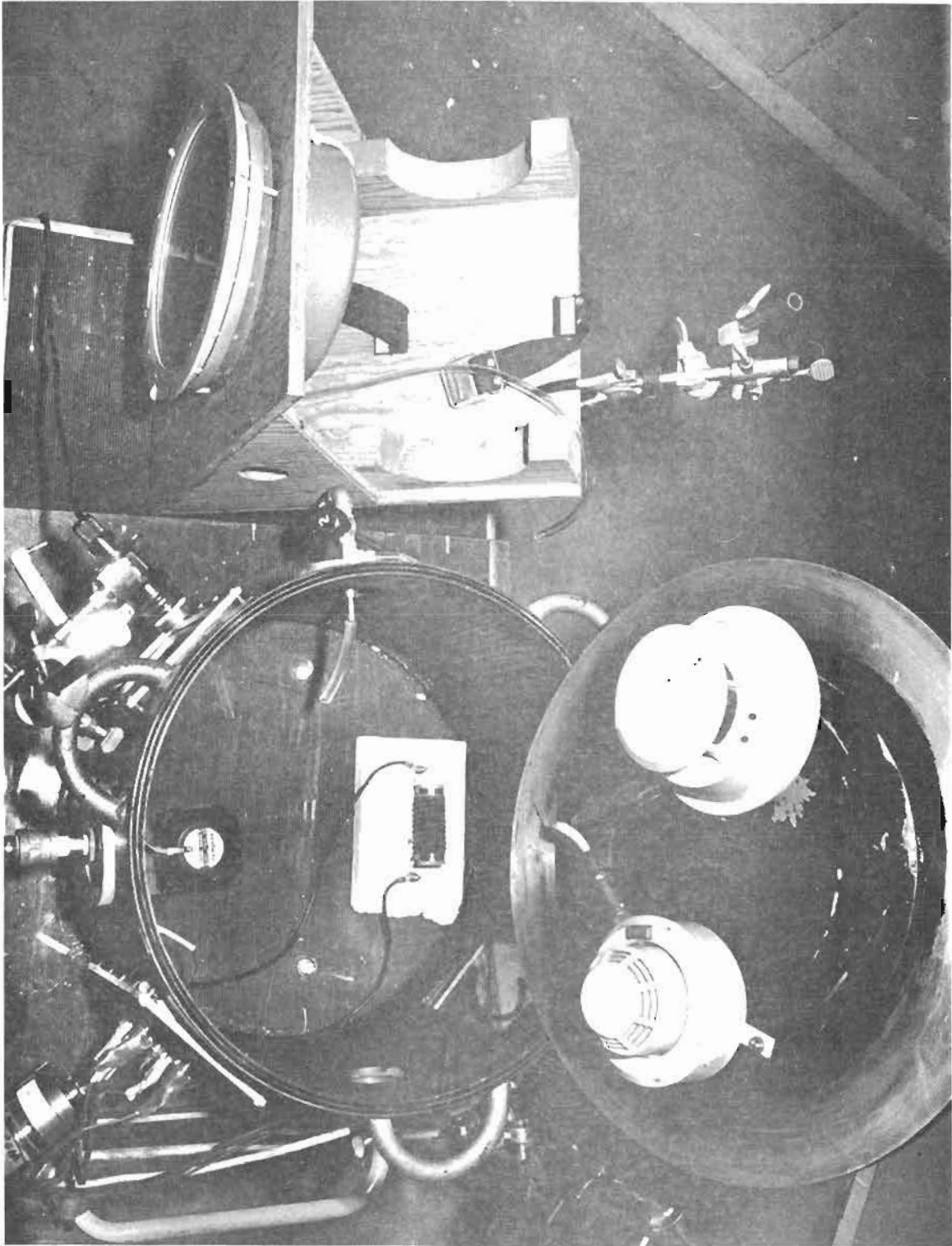
was between 120 and 135 cm/sec. Since the reproducibility and reliability of detectors D2, D5, D6, and D7 were quite good, we assume that a relatively constant ambient airflow rate will have only a minimal effect on first quality detectors.

Tests of the effect of ambient pressure and humidity on the response of the detectors were made by exposing both an ionization and a photoelectric detector (D6 and D5) to the pyrolysis products from a Group II smoldering cellulosic fuel in the apparatus shown in Figure 15. The data from these tests are presented in Table 12. Tests were conducted at a pressure of 1 atm (760 Torr) and 60% RH for the base line, 1 atm and 95.3% RH to test the effect of humidity; and 0.53 atm (480 Torr) and 60% RH to test the effect of pressure. These tests indicate that changes in relative humidity have little effect on the response of either of the detectors and that reduction in the pressure tends to reduce the sensitivity of the ionization detector only. Adjusting the electrical potential of the reference chamber enables the sensitivity of the ionization detector to return to its normal level. In both cases, the response of the photoelectric detector remained essentially constant.

### Conclusions

The data obtained from radiant heat, flame, and heated coil exposure tests indicate that:

- Both ionization and photoelectric detectors are equally capable of detecting the products of pyrolysis and combustion of synthetic polymers, especially those containing fire-retardant additives.
- No detector actuated before flaming ignition for cellulosic basic materials, and only ionization detectors appeared to be sensitive to the combustion products. Both ionization



SA-3830-14

FIGURE 15 PRESSURE AND HUMIDITY CHAMBER

Table 12

SELECTED DETECTORS AT ELEVATED HUMIDITY AND REDUCED PRESSURE

Materials	Order of Detector Actuation			Optical Density at which Detector Actuated			Chamber Conditions		
	First	Second	$\frac{\text{MAXOD}}{t \text{ MAXOD}}$	D5	D6	MAXOD	Relative Humidity	$P_{\text{ch}}^*$	$t_{\text{ch}}^\dagger$
50% Cotton/50% rayon fabric	D5	D6	$\frac{29.3}{0.016}$	0.016	0.021	0.055	Ambient $\approx 60\%$	760	42
			$\frac{30.9}{0.021}$						
50% Cotton/50% rayon fabric	D5	D6	$\frac{31.0}{0.031}$	0.031	0.175	0.377	Ambient $\approx 60\%$	480	61.7
			$\frac{44.4}{0.175}$						
50% Cotton/50% rayon fabric	D6	D5	$\frac{22.5}{0.002}$	0.014	0.002	0.050	95.3%	760	44.3
			$\frac{30.7}{0.014}$						

\*  $P_{\text{ch}}$  = Chamber pressure 10 Torr

$\dagger t_{\text{ch}}$  = Maximum chamber temperature  $10^\circ\text{C}$ .

and photoelectric detectors responded to products from smoldering or glowing cellulose.

- Detector D7 had the best repeatability in response to both individual materials and the actuation optical density; it was also consistently more sensitive than other scattering detectors.
- Detector D5 appears to have properties similar to those of D7, particularly after the manufacturer had repaired it.
- Detector D1 does not appear to be sensitive to pyrolysis or combustion products from the majority of the materials tested. However, the replacement detector functioned adequately during the radiant exposure tests with the Group III materials.
- Detector D9 appeared to function adequately during the radiant exposure tests with Group III materials. However, the detector and its replacement were both troubled with clogging of the pump vane during exposures to heavy smoke loads.
- Photoelectric detectors appear to have more tolerance in terms of exposure reliability to external perturbation such as air velocity, ambient pressure, and humidity effects. Since these detectors also are simpler in design and have adequate sensitivity to products of pyrolysis and combustion, they should be seriously considered for use in aircraft cabins.

## Appendix A

### SUGGESTED OVERALL PROGRAM FOR THE DEVELOPMENT OF FIRE DETECTORS FOR COMMERCIAL AIRCRAFT

#### 1. Phase I: Preliminary Evaluation of Current Detectors

Phase I consists of the following tasks:

- (1) Select contemporary smoke detectors<sup>\*</sup> such as ionization detectors, scattering-aerosol detectors, and gas analyzers that show promise for aircraft application.
- (2) Design and evaluate testing apparatus including:
  - Stagnation-flow, radial-symmetry enclosure.
  - Test parameters
    - Air temperature
    - Air velocity
    - Air pressure
    - Smoke composition<sup>+</sup>
  - Combustion mode
    - Pyrolysis
    - Smoldering
    - Flaming
  - Apparatus stability and recycle frequency

---

<sup>\*</sup>We restrict this discussion to smoke detectors (with emphasis on ionization and aerosol scattering sensors) since both electromagnetic and thermal detection concepts are infeasible in this application. By "smoke" we imply both vapor and aerosol products of combustion and pyrolysis

<sup>+</sup>This may have to be deferred during screening tests because of the expense.

- (3) Group tested material by polymer class.
- (4) Make screening tests (~ 40 materials, 3 cycles).
- (5) Select statistics to identify optimum contemporary detector, and install and test selected detectors in lavatory modules at University of California Fire Test Center, Richmond.
- (6) Continue survey for contemporary commercial detector systems compatible with the mission of project.

## 2. Phase II: Evaluation of Ambient Background of Aircraft Interiors

Phase II includes evaluation of aircraft ambient background in:

- Ventilation paths in aircraft cabin including:
  - Intake and outlet location
  - Air velocity spectrum (main cabin, lavatories, galleys, and same locations when occupied).
  - Individual seat vent nozzles.
- Cabin temperature range (when occupied and unoccupied).
- Cabin pressure range
- Cabin humidity
- Ambient air contamination (aerosol, dusts, smoke, canned sprays, perspiration and other body effluents, and polymer outgassing).

## 3. Phase III: Development and Testing of New Detector Concepts

Phase III should be a parallel effort with Phase II so that advantages and limitations can be checked simultaneously. Phase III includes:

- Qualitative analysis of major pyrolyzates from interior materials to assess and compare components of the pyrolyzates that could have similar detectable potential. (Some work has been advanced in the literature on determining toxic potential from major polymer classes. Advantage would be taken of these data.) A part of the NASA program is to ascertain biological

response to materials degradation and both the detector and biological response data should be integrated for study.

- Detector developing including:
  - Coincidence smoke scattering and ionization detection.
  - Detection of individual components of pyrolysis gases that are common to most combustion processes, such as CO, CO<sub>2</sub>, C<sub>n</sub>H<sub>m</sub>, and nitrogen- halogen- and sulfur-containing gases.
  - Remote sampling detectors. A conveniently located discrimination device coupled to a simple analyzer to trigger the alarm circuit. Sampling heads are located at hazardous areas and transmit an aliquot of gas to the discriminator. Examples of such discriminators are the mass spectrometer, nondispersive spectral sensor, catalytic conversion system, NASA heterodyne device for high specificity gas detection, and others, to be identified as more information becomes available about the component spectrum from smokes of interest.
  - Fullscale testing at University of California Fire Testing Facility at Richmond and/or testing in the proposed NASA fuselage section.

4. Phase IV: Installation of an Optimum Detector System on Commercial Aircraft for Flight Testing

## Appendix B

### SURVEY OF ACTUAL FIRE DETECTION IN AIRCRAFT FUSELAGE AREAS

In attempting to document actual experience with fire or combustion products detectors located in fuselage areas, we conducted an extensive literature search<sup>3</sup> and expended considerable effort in personnel and telephone contacts with individuals responsible for aircraft fire protection. We were essentially unsuccessful in uncovering any definitive information. Aircraft manufacturers and airline operators admitted to the existence of primarily photoelectric smoke detectors in cargo areas of most aircraft and in cargo and galley areas of wide-body jet aircraft, but until summer of 1975 no data were publicly available concerning detector performance either in terms of fire occurrence, detector reliability, or frequency of false alarm.

The detectors that had cornered approximately 95% of the aircraft market were those of Pyrotec used to detect scattering smoke. Models 30-284 and 30-284-2 with alarm sensitivities set at (7-10%) and (3-6%) transmission reduction. According to Pyrotec personnel, the sensitivity requirements of these detectors were specified by FAA. Their experience is summarized in Reference 4.

The only other information obtained about fire detection on aircraft are the results of tests with either optical (UV) or excess heat detectors to determine detector performance in engine nozzels.<sup>5</sup> Although the test results for optical detectors were encouraging, previous experience in the field indicated that engine detection systems were unreliable and that improved systems are needed for this application.

#### REFERENCES

1. G. Heskestad, "Escape Potentials from Apartments Protected by Fire Detectors in High-Rise Buildings," Technical Report, Serial No. 21017, Factory Mutual Research Corporation (June 1974).
2. J. P. Wagner, et al., "Fire Alert Systems for Metal and Non-Metal Mines," Final Report to Bureau of Mines, Contract No. SO 144131, Gillette Research Institute, Rockville, Md. (August 22, 1975).
3. G. V. Lucha, M. A. Robertson, and F. A. Schooley, "An Analysis of Aircraft Accidents Involving Fires," NASA CR 137690, Stanford Research Institute, Menlo Park, Calif. (May 1975).
4. "Product Installations," Pyrotector Incorporated, Hingham, Mass.
5. C. L. Delaney, "Fire Detection System Performance in USAF Aircraft," Technical Report AFAPL-TR-72-49, Wright-Patterson Air Force Base, Ohio (August 1972).